

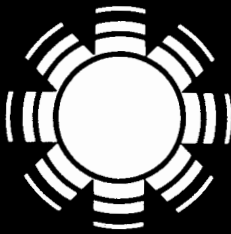
Measurements of Television Interference Caused by a Vertical Axis Wind Machine

Final Subcontract Report

Dipak L. Sengupta
Thomas B. A. Senior
Joseph E. Ferris

Radiation Laboratory
Department of Electrical and
Computer Engineering
University of Michigan

Prepared Under Subcontract No. XH-0-9263-1



SERI

Solar Energy Research Institute

A Division of Midwest Research Institute

1617 Cole Boulevard
Golden, Colorado 80401

Operated for the
U.S. Department of Energy
Under Contract No. EG-77-C-01-4042

Printed in the United States of America
Available from:
National Technical Information Service
U.S. Department of Commerce
5285 Port Royal Road
Springfield, VA 22161
Price:
Microfiche \$4.50
Printed Copy \$11.50

NOTICE

This report was prepared as an account of work sponsored by the United States Government. Neither the United States nor the United States Department of Energy, nor any of their employees, nor any of their contractors, subcontractors, or their employees, makes any warranty, express or implied, or assumes any legal liability or responsibility for the accuracy, completeness or usefulness of any information, apparatus, product or process disclosed, or represents that its use would not infringe privately owned rights.

SERI/STR-215-1881
UC Category: 60

**Measurements of Television
Interference Caused by a
Vertical Axis Wind Machine**
Final Subcontract Report

Dipak L. Sengupta
Thomas B. A. Senior
Joseph E. Ferris

Radiation Laboratory
Department of Electrical and
Computer Engineering
University of Michigan

January 1983

Prepared Under Subcontract No. XH-0-9263-1

SERI Technical Monitor: Neil Kelley

Solar Energy Research Institute

A Division of Midwest Research Institute

1617 Cole Boulevard
Golden, Colorado 80401

Prepared for the
U.S. Department of Energy
Contract No. EG-77-C-01-4042

ABSTRACT

The electromagnetic interference to television reception caused by the 17 m Darrieus at Albuquerque, NM, has been studied by carrying out measurements at a number of sites in the vicinity of the VAWT. The RF sources used were the commercial VHF and UHF TV signals available in the area.

Ambient field strength measurements showed that the signals on all TV Channels except one were strong, and provided good reception at all test sites. With the antenna (properly) oriented for maximum direct signal, unacceptable interference was observed on some Channels at sites out to 33 m from the WT in the forward and backward regions. With the antenna beam directed at the WT, interference varying from slight to violent were observed at all sites on some or all TV Channels.

A simple theoretical model has been developed for analyzing the TVI produced by a VAWT like the Darrieus. Using the model in conjunction with measured data, an approximate expression for the equivalent scattering area A of the Darrieus has been developed. It is found that A is wavelength (λ) dependent and varies as $\lambda^{1/2}$. The equivalent scattering area of the Darrieus on low VHF Channels is found to be of the same order as that of a HAWT having a similar power rating. It appears that the Darrieus produces the same amount of interference on the lower VHF Channels but less on all others. The modulation waveforms produced by the Darrieus are more complicated than for a horizontal axis machine and are not yet fully understood.

EXECUTIVE SUMMARY

Electromagnetic interference to television reception caused by the 17 m Darrieus at Albuquerque, NM, has been studied by carrying out measurements at a number of sites in the vicinity of the WT. The RF sources used were the commercial TV signals on VHF Channels 4,5,7 and 13, and UHF Channels 23 and 48 available in the area. The transmitters of all six are located on Sandia Crest (approximately 3.2 km above sea level) about 21 km from the WT. Eight test sites at various distances from the WT were chosen in directions having angles measured clockwise from the WT-transmitter direction as follows: one site in the backward direction (0°), two sites in the forward (180°) direction, one site each in the 45° and 135° directions, and three sites in the 90° direction. Seven of these were located within 45 m of the WT, close to the surrounding fence, and the eighth (in the 90° direction) was outside the VAWT control building about 133 m from the WT.

At each site some or all of the following types of measurement were performed:

(i) Ambient Field Strength. With the WT stationary, the strength of the received signal was measured by rotating the main beam of the receiving antenna until the output was a maximum. This provided information about the expected quality of TV reception in the area, and also the average field strengths of the various TV Channels at the WT relative to those at the test sites. The latter are important in predicting the interference produced by the WT.

(ii) Dynamic or Television Interference (TVI). These tests were performed with the WT rotating (at 50.6 rpm) by recording the received signal vs. time with the antenna beam directed at the desired transmitter or at the WT, while observing the received picture on the screen for any video distortion. Video recordings were made whenever it was felt desirable to preserve the video effects for future evaluation. In addition, the received signal vs. antenna beam pointing direction was obtained for each TV Channel. These measurements provided substantial information, and were used to judge the following: (a) the horizontal plane pattern of the antenna in the actual test environment under dynamic conditions; (b) the effect of the WT and/or its blade rotation on the signal received from any direction, and (c) the amount of signal modulation caused by the blade rotation. At one site (#7) a photograph of the oscilloscope display of the modulation waveform on Channel 13 was obtained for future analysis.

The equipment setup and the measurement procedures were similar to those employed in our previous studies. The receiving antenna was a typical TV antenna purchased from a Radio Shack store in Albuquerque.

The ambient field strength measurements showed that in the vicinity of the VAWT the signals on all TV Channels except 23 were strong enough to provide good reception at all of the test sites. The Channel 23 signal was generally weak, and its reception was considered poor at all sites.

With the antenna beam directed at the transmitters (i.e., the antenna properly oriented), the significant findings from the dynamic measurements were: (i) in the forward direction (180°), threshold level video distortion was observed on Channels 23 and 48 at a distance of 33 m from the WT; (ii) in the backward direction (0°) there was no video distortion on any Channel at a distance of about 37 m; (iii) at the sites in the 90° direction 21 and 23 m from the WT, unacceptable video distortion occurred on Channel 23; and (iv) at two sites 23 m from the WT and in the 45° and 135° directions, there was interference above acceptable levels on Channels 13 and 23, respectively.

With the antenna beam directed at the WT (i.e., antenna improperly directed for backward region sites), interference ranging from slight to violent was observed on some or all Channels at all eight sites.

The modulation waveforms produced by the rotating Darrieus were more complicated than for a HAWT and are not fully understood. The waveforms varied from sinusoidal to pulsed, with significant components repeating at twice the rotation frequency of the blades. The video distortion occurred in synchronism with these components.

A simple theoretical model has been developed for analyzing the TVI produced by a VAWT like the Darrieus. Using this model and the measured data, an approximate expression for the equivalent scattering area A of the 17 m Darrieus has been derived. It is found that A is wavelength (λ) dependent and varies at $\lambda^{1/2}$. The equivalent area of the Darrieus on low VHF Channels is found to be of the same order as that for a HAWT having similar power rating. It appears that the

Darrieus produces the same amount of interference on the lower VHF Channels but less on all other Channels.

The test program was successful, and yielded valuable information and understanding of the TVI effects caused by the Darrieus. Further work is recommended so that the interference phenomenon associated with a Darrieus or other VAWT can be understood with the same degree of confidence now possible for a HAWT.

TABLE OF CONTENTS

	<u>Page</u>
NOTICE	i
ACKNOWLEDGEMENTS	ii
EXECUTIVE SUMMARY	iii
CHAPTER 1. INTRODUCTION	1
CHAPTER 2. BACKGROUND INFORMATION	3
2.1 Description of the Darrieus VAWT	3
2.2 Physical Environment	5
2.3 TV Stations	8
2.4 TV Interference Phenomenon	9
2.5 Test Sites	12
CHAPTER 3. EXPERIMENTAL ARRANGEMENT AND DESCRIPTION OF MEASUREMENTS	15
3.1 Experimental Setup	15
3.2 The Receiving Antenna	17
3.3 Types of Measurement	32
CHAPTER 4. MEASURED AMBIENT FIELD STRENGTHS	35
CHAPTER 5. DYNAMIC ANTENNA RESPONSE	39
CHAPTER 6. TELEVISION INTERFERENCE (TVI)	53
6.1 Forward Region Interference	53
6.2 Backward Region Interference	58
6.3 Theoretical Considerations	70
6.4 Data Analysis	74
6.5 Comparison with a HAWT	78
CHAPTER 7. CONCLUDING REMARKS	80
REFERENCES	83

CHAPTER 1. INTRODUCTION

Vertical axis wind turbines are a possible alternative to the more conventional horizontal axis machines for wind energy conversion, and a number have been erected or are in the process of erection throughout the U.S. Like horizontal axis machines, they are also a potential source of interference with electromagnetic systems operating in the vicinity, and television is one type of system that could be affected.

To date, most studies have been directed at large horizontal axis wind turbines (HAWTs) such as the MOD-0A and MOD-1, and it has been demonstrated [1,2] that these can interfere with television reception in a neighborhood of the site. The television interference (TVI) is due to scattering off the rotating blades of the turbine, producing pulse amplitude modulation of the total received signal, and manifests itself as video distortion of the received picture. Depending on the location and orientation of the receiving antenna and the state of the wind turbine (WT), the amount of observed video distortion can range from weak (or acceptable) to very strong (or unacceptable). It has been found that in the worst case the MOD-1 WT at Boone, NC, can produce unacceptable interference out to 4 to 5 km from the machine.

A preliminary investigation [3] using a laboratory microwave TV system and scale models of vertical axis wind turbines (VAWTs) showed that the Giromill and Darrieus can cause TVI. Although the general nature of the interference was similar to that of a horizontal axis machine, there were some differences in magnitude and detail, but the

study was limited in extent and simulated only a single UHF TV Channel. It is therefore of interest to examine the nature and severity of the TVI caused by a full scale VAWT in an actual (as opposed to laboratory) environment. To this end, a series of on-site measurements was carried out during the period 10-14 November 1980 using the 17 m Darrieus machine at the Sandia Laboratories in Albuquerque, NM. The specific objectives were to measure the form and magnitude of the interference to actual TV signals caused by a full scale VAWT, and to compare them with those for a comparable HAWT. The tests were conducted by receiving the commercial TV signals available at selected sites in the vicinity of the machine. The following chapters describe these on-site measurements, and discuss the results and their implications.

CHAPTER 2. BACKGROUND INFORMATION

2.1 Description of the Darrieus VAWT

Figure 1 shows a photograph of the 17 m Darrieus in its two-bladed configuration. It is located at the NE corner of Kirtland Air Force Base on the west side of the Sandia Mountains in New Mexico. The blades and the central supporting torque tube (tower) form the rotating part of the turbine referred to as the rotor. The unique feature of the turbine is the special shape of the blade formed by straight-circular-straight blade sections that approximate a troposkein curve (the shape that a perfectly flexible blade would assume under centrifugal forces) [4,5]. The blades are of NACA-0015 aerofoil section and are pin-attached at all points including the central rotating steel tower, which is supported at the top and bottom by tapered roller bearings. The metallic blades are uniformly 24 inches wide and have a chord thickness of 3.6 inches over their entire length. Four guy cables attached to the housing of the top bearing provide the necessary tower support. Visible in Fig. 1 is a slender pole projecting from the top bearing which holds anemometers and wind direction sensors to record the wind conditions near the turbine during testing. The relevant parameters of the Darrieus shown in Fig. 1 are presented in Table 1. More details about the WT can be found in [4,5].

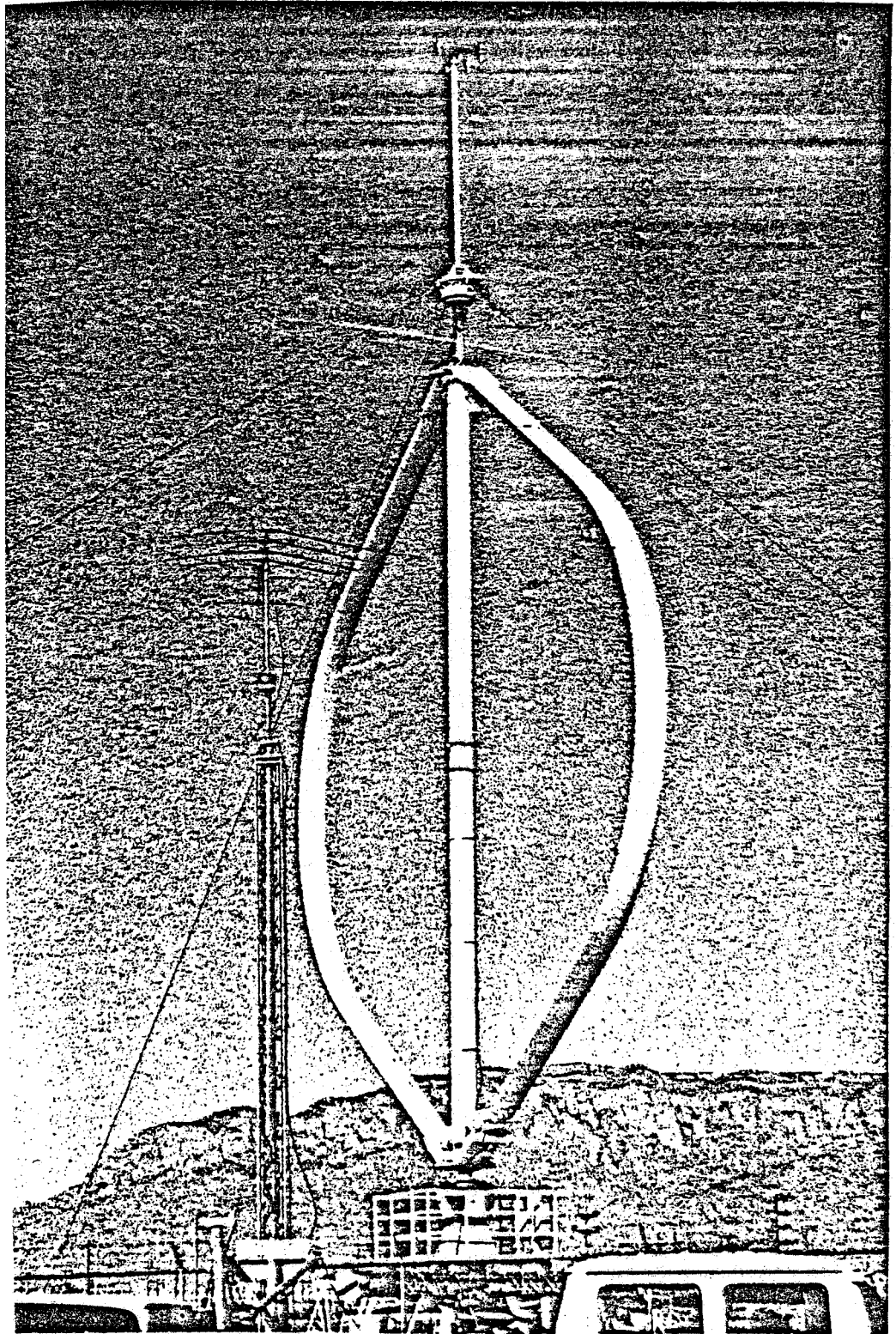


Fig. 1: The 17 m Darrieus machine.

Table 1
Relevant Parameters of the Darrieus at Albuquerque, NM

Rotor Diameter	17 m (54.9 ft)
Total Height	28.7 m (94 ft)
Total Weight	37,000 lbs
Aerofoil Section	NACA 0015 with 2 ft chord
Rated Power	50 kw with 2 blades at 50.6 rpm and 28.7 mph wind
Peak Turbine Efficiency	41 percent

2.2 Physical Environment

The turbine is located on a flat section of ground at an elevation of 5,450 ft above sea level. The immediate vicinity of the turbine site, and a section of the U.S. Geological survey map of the larger region surrounding the turbines are shown in Figs. 2 and 3. As seen from Fig. 2, the 17 m Darrieus is surrounded by a metallic (security) fence about 150 ft square, and there are also two smaller Darrieus machines 5 m and 2 m in diameter about 260 and 400 ft away respectively in the SE direction from the WT under test.

The area available for carrying out the measurements extended out about 0.5 mile from the WT and was circular apart from the region to the west occupied by Kirtland Air Force Base. The only other major obstructions in the area were two tall water towers and a metallic tower about 500 ft away in a northerly direction.

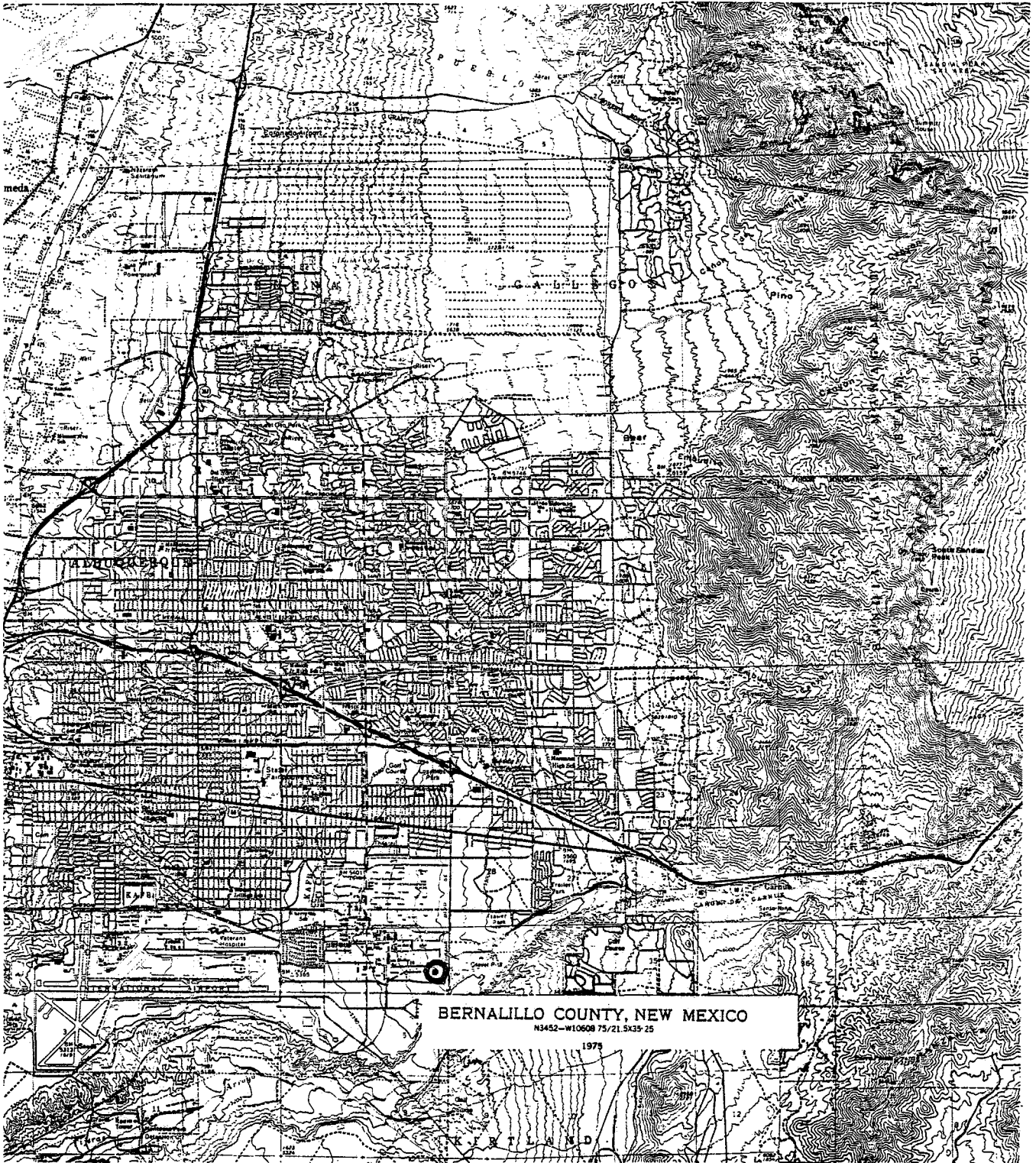


Fig. 3: U.S. Geological Survey map of the area showing the WT site (O) and the Sandia Crest (X) where the TV transmitters are located.

2.3 TV Stations

Four VHF and two UHF commercial TV signals could be received in the area. Their transmitters are all located on Sandia Crest (10,600 ft above sea level) which is 12.7 miles from the WT in a direction 10° east of magnetic north (2° west of true north). Information concerning the TV transmissions is given in Table 2, where the blanks indicate that the data was not available. It is understood that the Channel 48 transmission is a re-broadcast of a satellite-received signal.

Table 2
 Available TV Channels in Albuquerque, NM
 (Transmitting Antennas: 12.7 miles from the WT)

TV Channel and Affiliation	Audio Carrier Freq. Wavelength		Peak Effective Radiated Power (kw)	
	(MHz)	(m)	Video	Audio
4 KOB NBC	71.75	4.2	27.0	2.7
5 KNME EDU	81.75	3.7	26.9	5.4
7 KOAT ABC	179.75	1.7	89.0	17.8
13 KGCM CBS	215.75	1.4	89.0	---
23 ---	529.75	0.6	922.0	184.0
48 ---	679.75	0.4	22.0	2.8

2.4 TV Interference Phenomenon

To better appreciate the tests and the results to be described later, it is convenient to begin with a general description of TV interference near a large horizontal axis WT [1,2,6,7]. It is natural to expect that the gross character of the interference produced by a VAWT will be similar to this, but differences can also be anticipated. After all, the Darrieus is a very different physical structure, and some information which is relevant to the Darrieus and was obtained from our previous laboratory study [3] will also be given.

The rotating blades of a horizontal axis WT can interfere with TV reception by producing video distortion. At a given distance from the WT the interference increases with increasing frequency, and is therefore worse on the upper TV Channels. It also decreases with increasing distance from the machine. For ambient (primary) signals well above the noise level of the receiver, there is little or no dependence on the ambient field strength, and no audio distortion has been found.

The interference is caused by the time-varying amplitude modulation of the received signal produced by the rotating blades. In a neighborhood of a WT the signals scattered by the blades combine with the primary signal to create a form of time-varying multipath, thereby amplitude modulating the total received signal. With a horizontal axis WT having two distinct (coned) blades, each blade contributes separately, and the modulation waveform generally consists of sinc pulses whose width is inversely proportional to the electrical length of a blade, repeating at twice the rotation frequency of the blades. If sufficiently strong, these extraneous pulses can distort the received picture, whereas the audio

information, being transmitted by frequency modulation, remains unaffected.

Generally, the nature of the observed interference depends on the location of the receiver with respect to the WT, the state and orientation of the blades, and the direction of arrival of the primary signal. When the WT blades are stationary, the scattered signal may appear on the TV screen as a ghost whose position or separation from the main picture depends on the difference between the time delays suffered by the primary and scattered signals. A rotation of the blades then causes the ghost to fluctuate, and if the ghost is sufficiently strong, the resulting interference can be quite objectionable. In such cases, the received picture displays a horizontal jitter in synchronism with the blade rotation. As the interference increases the entire picture shows a pulsed brightening, and still stronger interference can disrupt the TV receiver's vertical sync, producing picture break-up. This type of interference occurs when the interfering signal reaches the receiver primarily as a result of specular scattering off the broad faces of the blades, and is called backward region interference. In the forward scattering region when the WT is almost in line between the TV transmitter and the receiver, there may be little or no difference in the times of arrival of the primary and scattered signals at the receiver, and the video distortion then appears as an intensity (or brightness) fluctuation of the picture in synchronism with the blade rotation. This type of interference is termed forward region interference. In both cases, the amount of interference depends on the strength of the scattered signal relative to the primary one, and this decreases with increasing distance

from the WT. The backward region interference shows no significant dependence on the ambient signal strength and appears to be independent of the receiver if the signal is well above the noise level of the receiver. In the forward region, however, the interference does depend on the ambient signal strength, and a receiver located in a low signal level area is more vulnerable to this type of interference.

The amount of video distortion observed depends on the ratio of the scattered and ambient field strengths at the input of the receiver, i.e., on the modulation index m of the total received signal, and the modulation threshold m_0 is defined to be the largest value of m for which the distortion is still judged to be acceptable. The threshold is obviously somewhat subjective, but as a result of laboratory simulations [7], scale model measurements [3] and field tests using the MOD-0 machines at Plum Brook [7] and on Block Island [1], it has been established as 0.15 for a receiver in the backscattering direction from the WT, increasing to 0.35 for a receiver in the forward scattering direction. The latter value is for strong ambient signals and could be as small as 0.15 in a low signal area. With the WT blades oriented to direct the maximum scattered signals to the receiver, the region where $m > m_0$ is defined as the interference zone whose shape is determined by the horizontal plane scattering pattern of a blade. A method for computing the interference zone of large horizontal axis WT is described in [8,9].

Most of the above comments also apply to the interference caused by a VAWT like the Darrieus, but there are differences in detail. In particular, our laboratory study [3] showed that the modulation waveform

introduced by a Darrieus contains broad pulses and narrow spikes, both repeating at twice the blade rotation frequency. The pulses produced video distortion with a threshold $m = 0.28$, but the spikes did not produce any observable distortion.

2.5 Test Sites

The measurements were carried out at eight test sites at various distances and directions from the WT. The locations of the sites are shown in Fig. 4. The farthest (site 1) was outside the WT control building (building No. 899) 450 ft east of the WT. The remaining seven sites were all within or just outside the fenced area around the machine. The distances r of the sites from the WT and their directions θ in degrees measured clockwise from the direction of the Sandia Crest (10° east of magnetic north) are listed in Table 3. Since $\theta = 0$ is the (common) direction of the TV transmitters, the sites can also be characterized as regards their position in an interference zone: see Table 4. We note that sites 6, 4 and 1 were all located approximately on the 90° radial from the WT-transmitter direction, but at increasing distances from the machine.

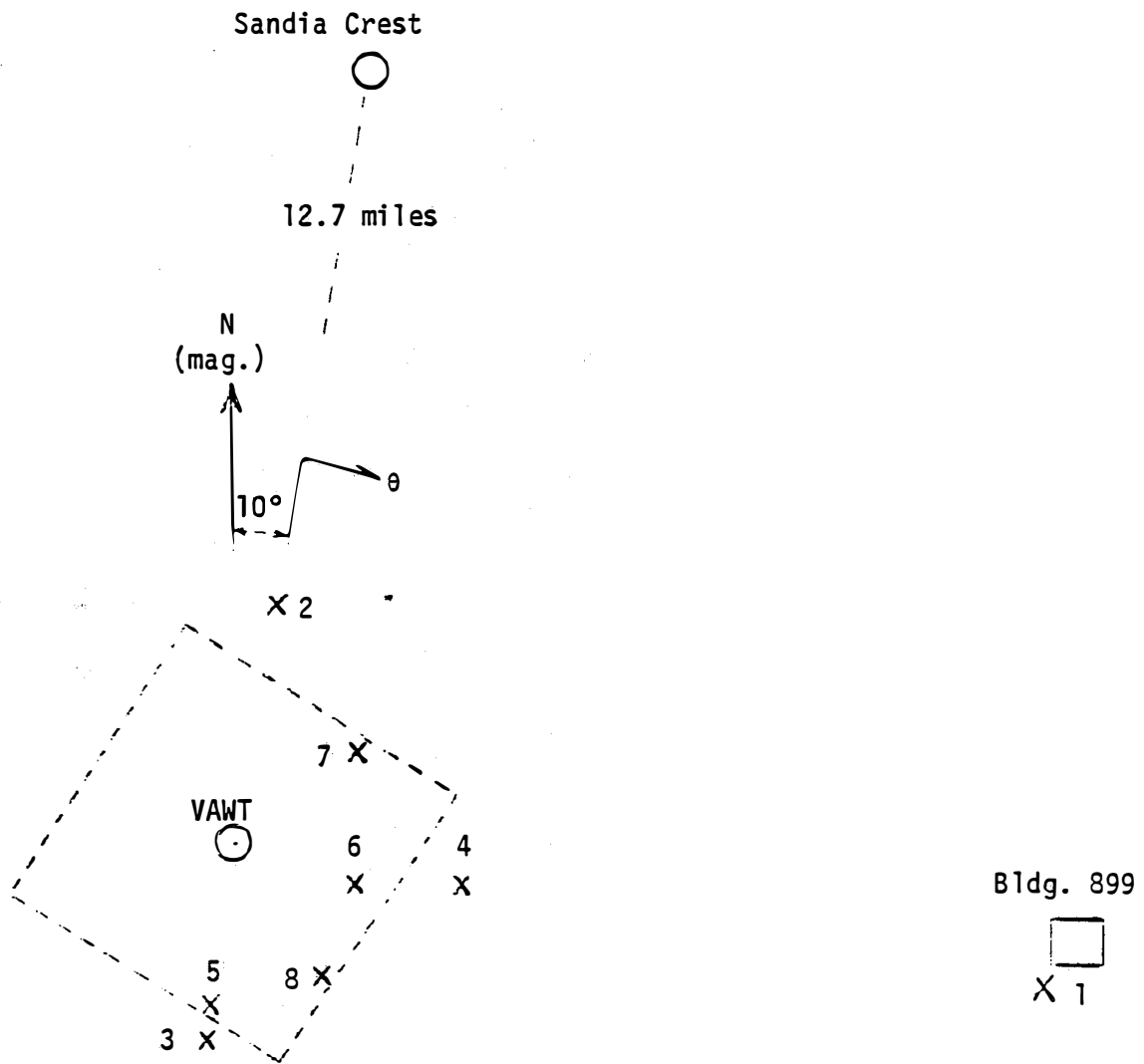


Fig. 4: Geometry of the test sites.

Table 3

Coordinates of the Test Sites with Respect to the Darrieus

Site No.	Distance r (in feet)	Angle θ (in degrees)
1	437	90
2	123	0
3	103	180
4	109	90
5	88	180
6	68	100
7	78	45
8	74	135

Table 4

Characterization of Test Sites for Interference

Site No.	Location
2	back scattering direction (almost exactly)
3,5	forward scattering direction (almost exactly)
1,4,6,7,8	backward interference region

CHAPTER 3. EXPERIMENTAL ARRANGEMENT AND DESCRIPTION OF MEASUREMENTS

3.1 Experimental Setup

The equipment used to perform the measurements was similar to that of our previous TVI tests [1,2]. A schematic block diagram of the system is shown in Fig. 5 where only those components pertinent to the data collection have been included. With any given TV transmitter, a portion of the signal is scattered by the WT and this, together with the desired signal, was picked up by an antenna and fed to a spectrum analyzer and a TV receiver. The receiving antenna, to be described later, was a commercially available directional antenna located 25 ft above ground.

The vertical output of the spectrum analyzer was connected to a chart recorder which provided a record on paper tape for later evaluation. The combination of the spectrum analyzer and the recorder was used to measure the ambient levels of the received video and audio signals without the WT in operation, and to record the total signal received as a function of time, including any modulation produced by scattering from the operating WT. The general quality of the ambient TV reception and the existence of any WT-produced video distortion were observed on the screen of a 17-inch Zenith TV receiver, and the video recorder was employed whenever it was felt desirable to record the program. In some special cases, the combination of the oscilloscope and camera (shown dotted in Fig. 5) was used to photograph the modulation waveform of the received signal. The test instruments were powered from a commercial 60 Hz power supply available at all of the test sites.

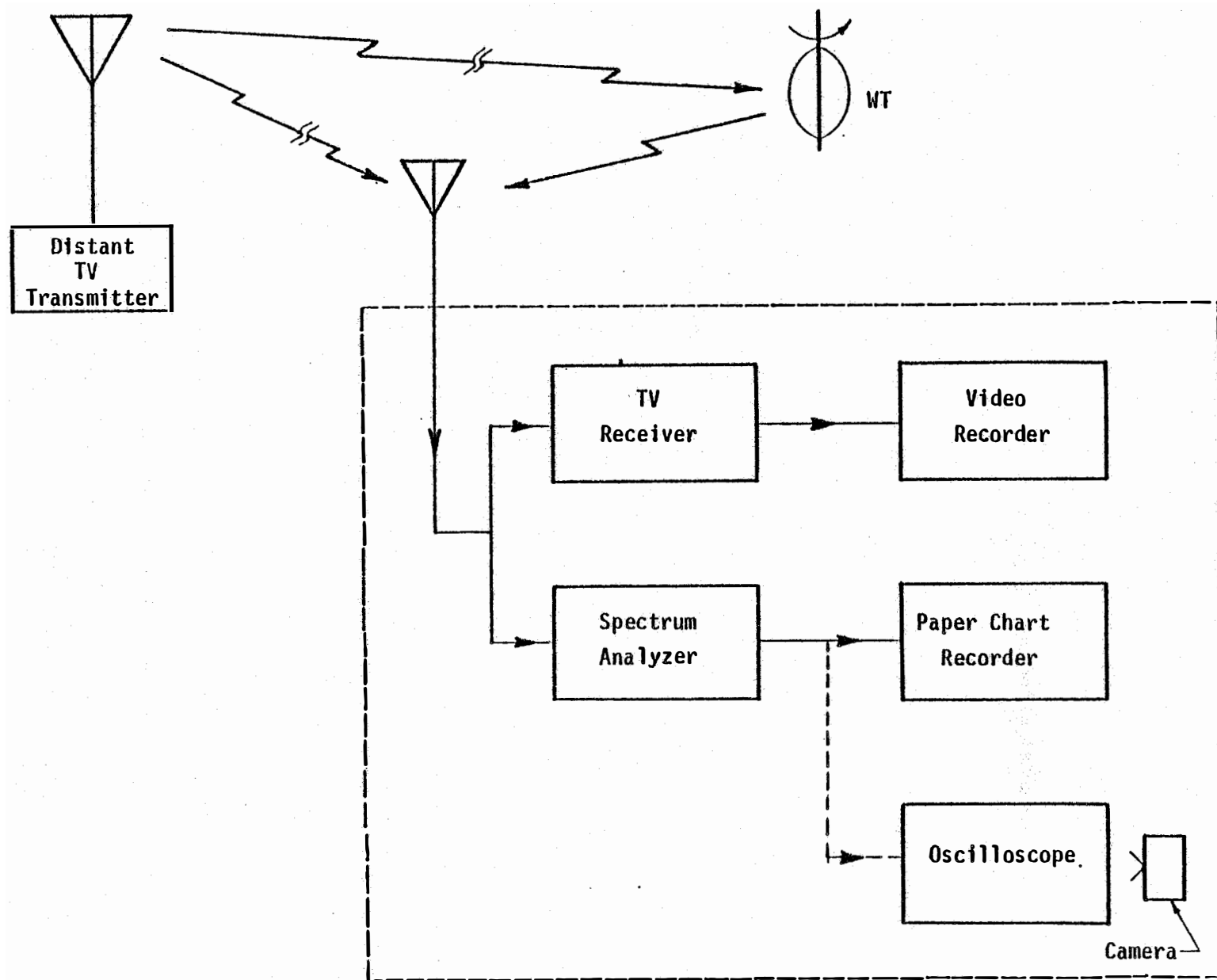


Fig. 5: Schematic block diagram of the measurement system.

All the test instruments fitted comfortably inside a van. The antenna was rotatable in azimuth and was mounted on a tower whose height was adjustable from 25 to 50 ft, as shown in Fig. 6. The tower and the antenna were mounted on a bracket assembly resting on four wheels so that the combination could be readily moved (see Fig. 7).

The Sandia Laboratories provided us with a van in which the test equipment was housed, and a pickup truck for moving the antenna and tower assembly. The combination of the van and truck served as a mobile laboratory for carrying out the measurements. The spectrum analyzer, paper chart recorder, video recorder, oscilloscope and camera were all provided by the Sandia Laboratories.

3.2 The Receiving Antenna

The receiving antenna was an Archer Model VU60 purchased from a Radio Shack Store in Albuquerque, and was a typical VHF/UHF antenna, basically of log-periodic design. For the appropriate TV Channel frequencies, the azimuth and elevation plane patterns were subsequently measured at our Willow Run Facility and are presented in Figs. 8 through 13. The calibration marks on the azimuthal patterns correspond to a gain of 2 dB above isotropic, and from these the gain of the receiving antenna can be found for each TV Channel.

At all of the test sites the horizontal (azimuth) plane patterns of the antenna were measured in the actual test environment by recording the antenna response as a function of the beam pointing direction. Typical of the results obtained are those shown in Figs. 14 through 19 for site 1, and these should be compared with the corresponding patterns in Figs. 8 through 13.

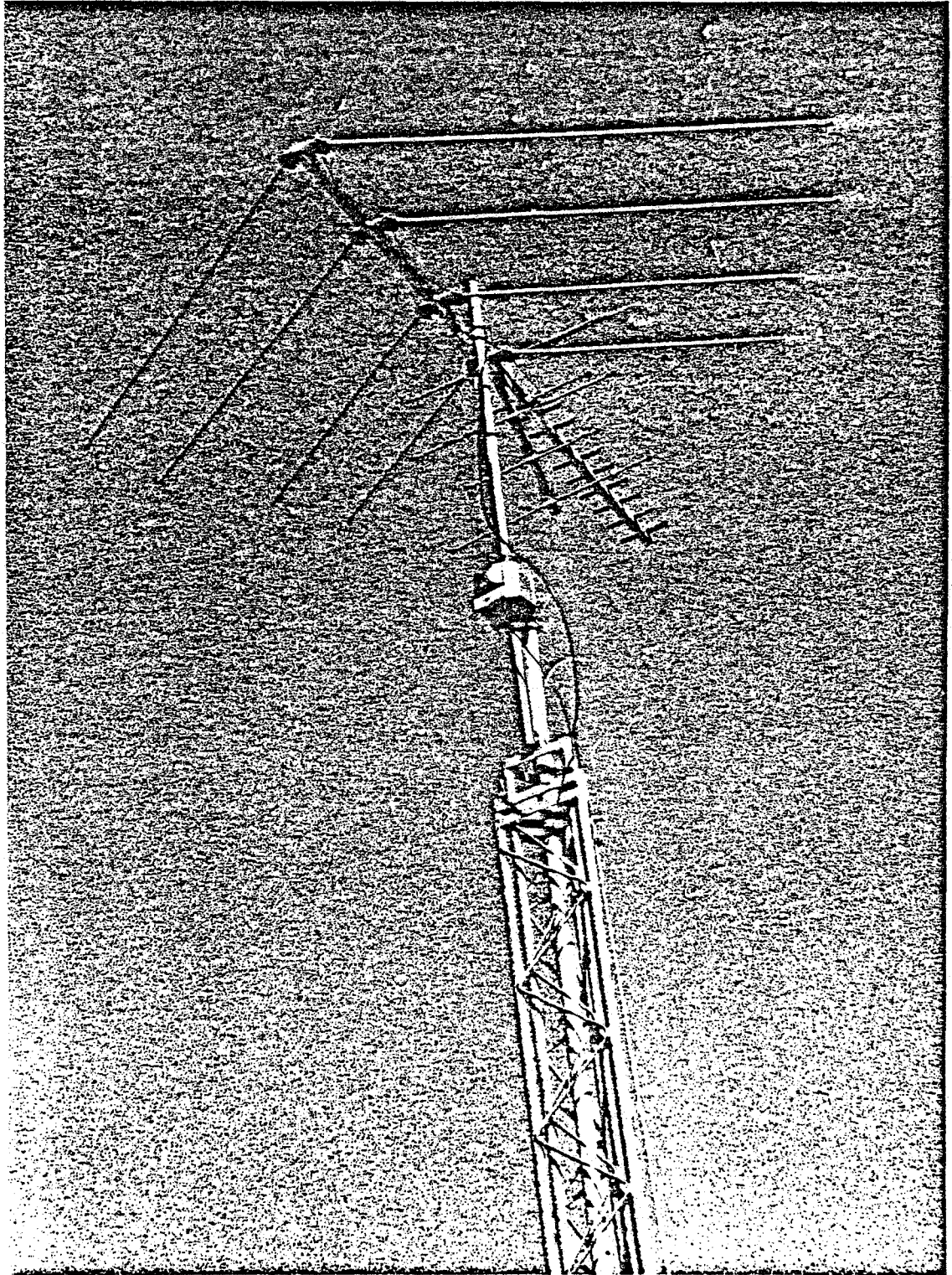


Fig. 6: Antenna mounted on the tower.

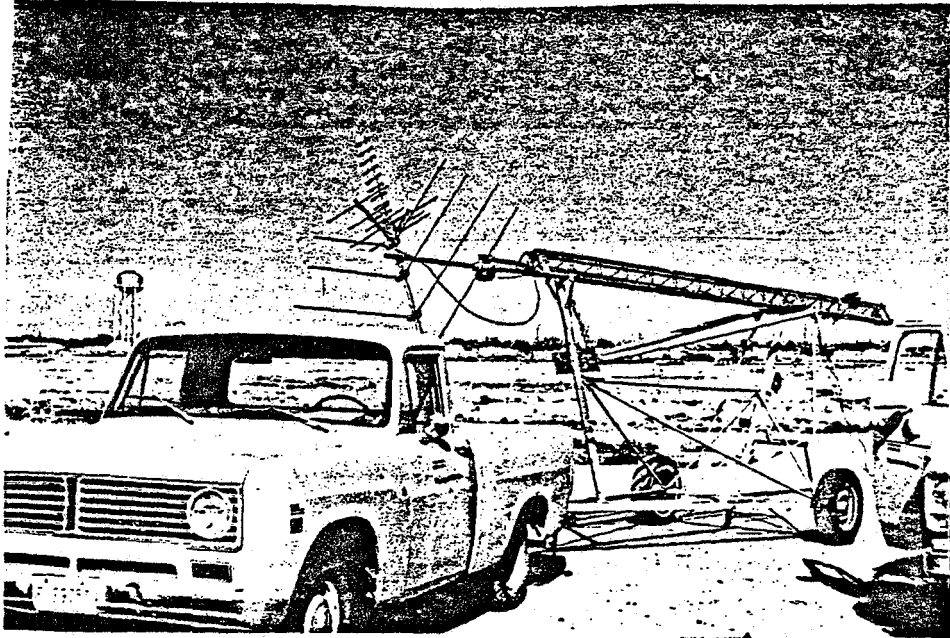


Fig. 7: Antenna and its tower stowed for movement from site to site.

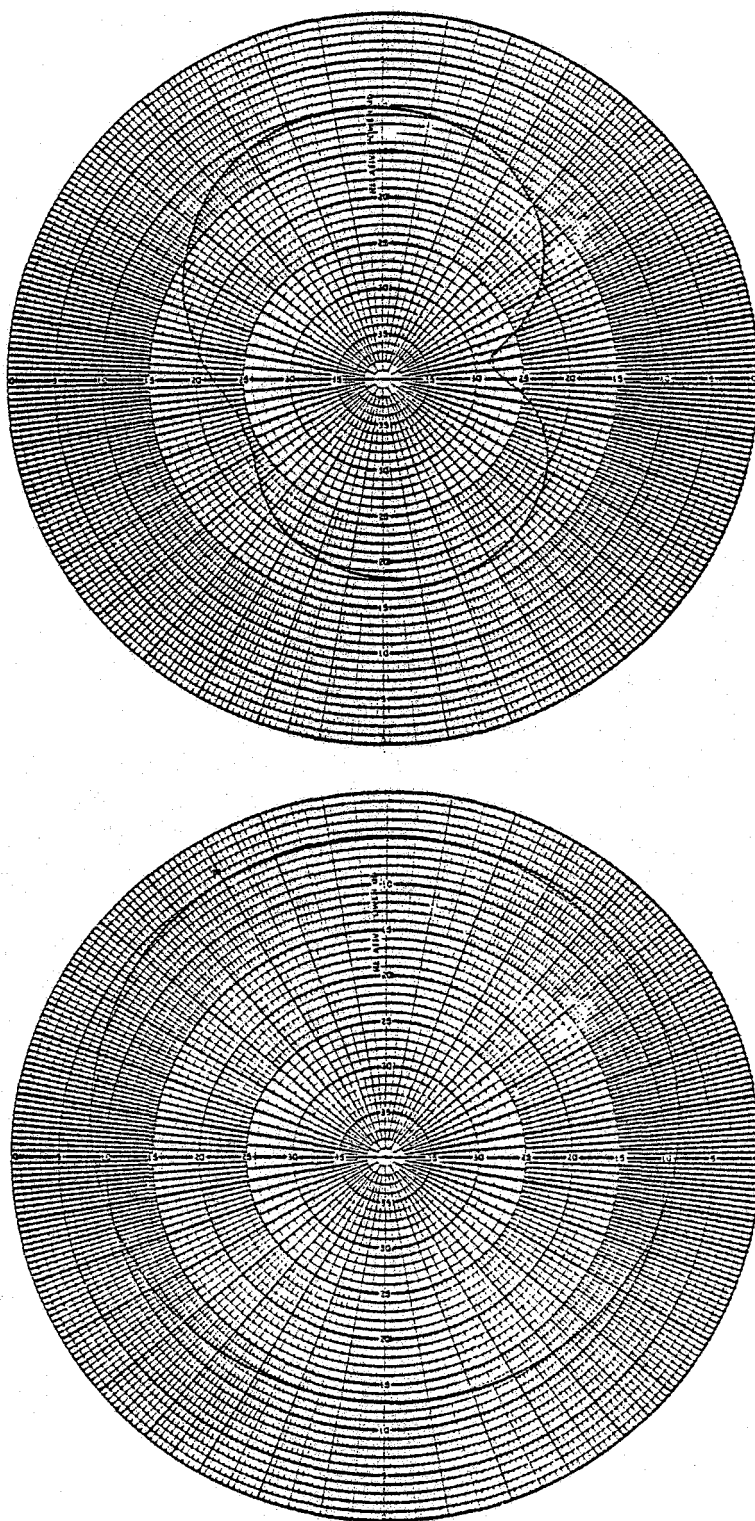


Fig. 8: Azimuthal (top) and elevation (bottom) plane patterns of the Radio Shack (VU60) receiving antenna at 69 MHz (Channel 4).

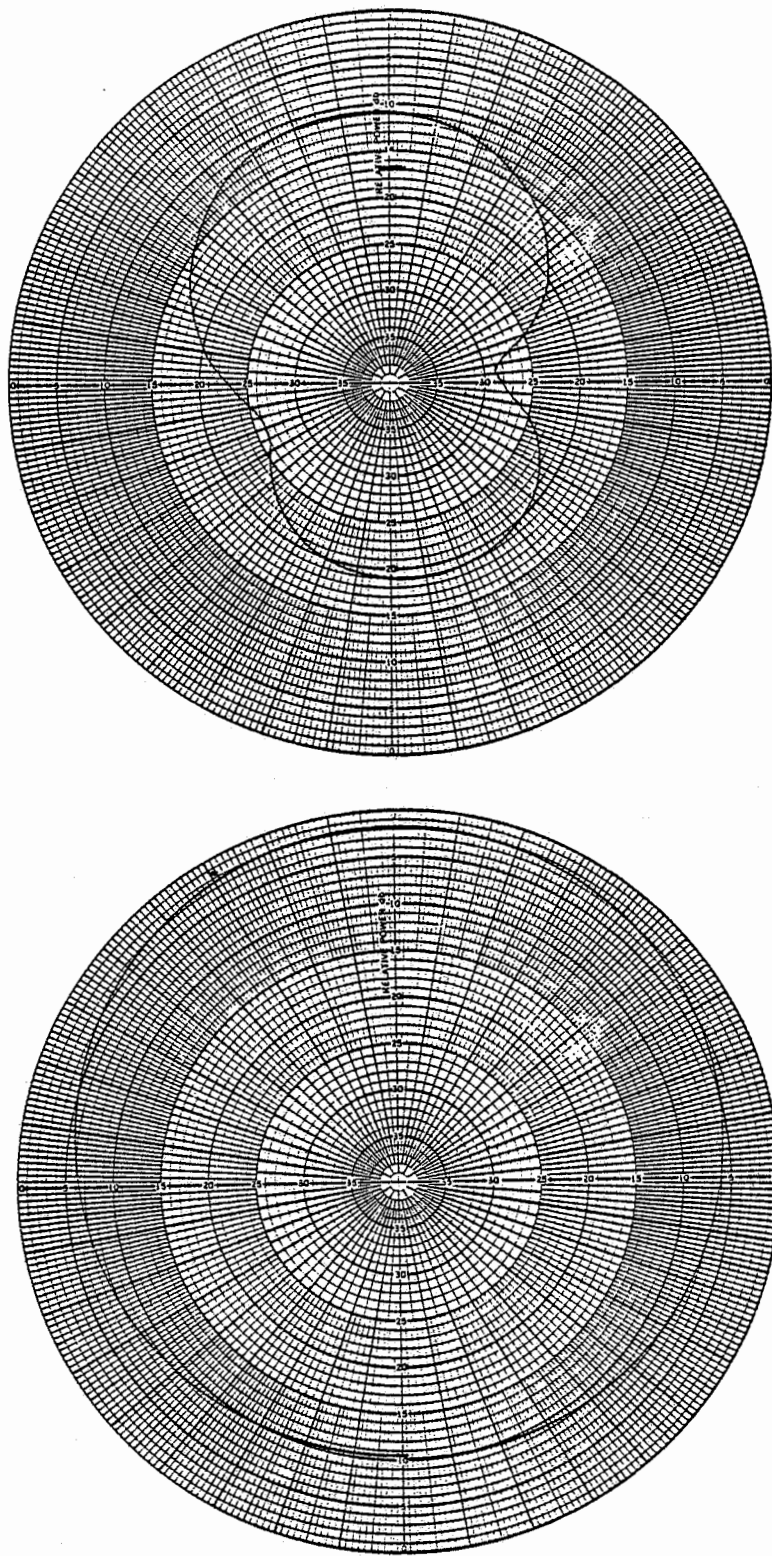


Fig. 9: Azimuthal (top) and elevation (bottom) plane patterns of the Radio Shack (VU60) receiving antenna at 79 MHz (Channel 5).

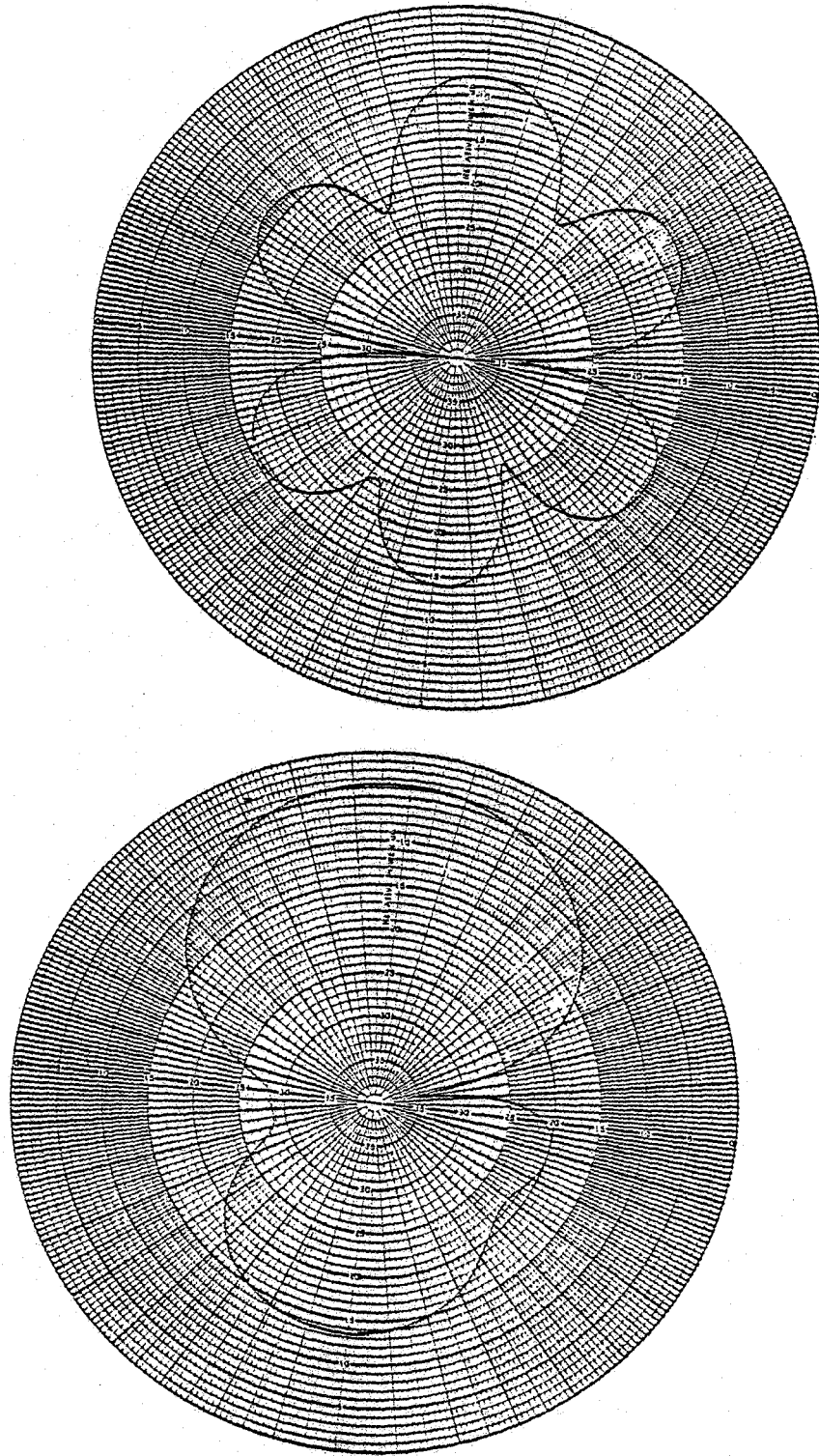


Fig. 10: Azimuthal (top) and elevation (bottom) plane patterns of the Radio Shack (VU60) receiving antenna at 177 MHz (Channel 7).

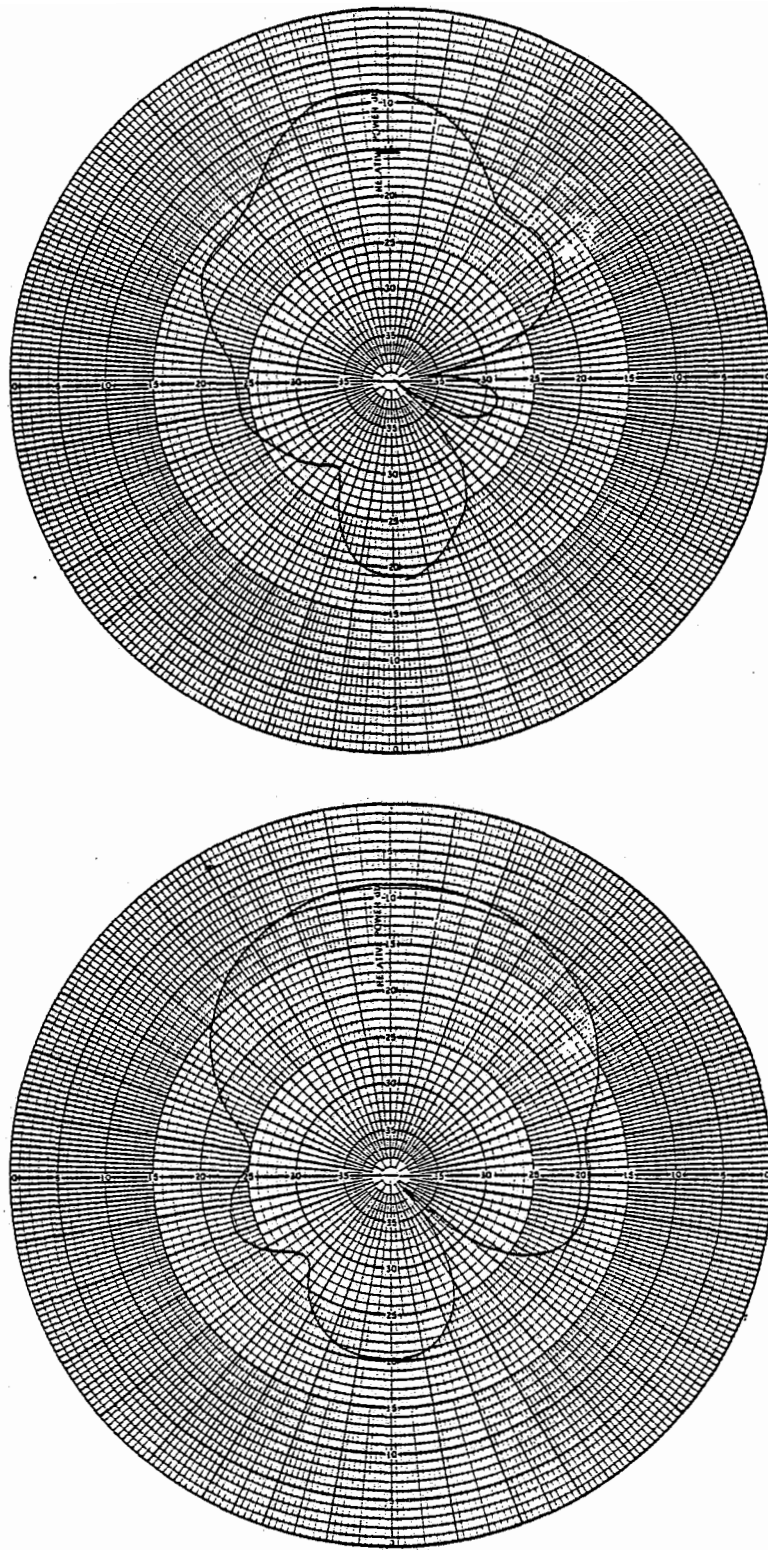


Fig. 11: Azimuthal (top) and elevation (bottom) plane patterns of the Radio Shack (VU60) receiving antenna at 213 MHz (Channel 13).

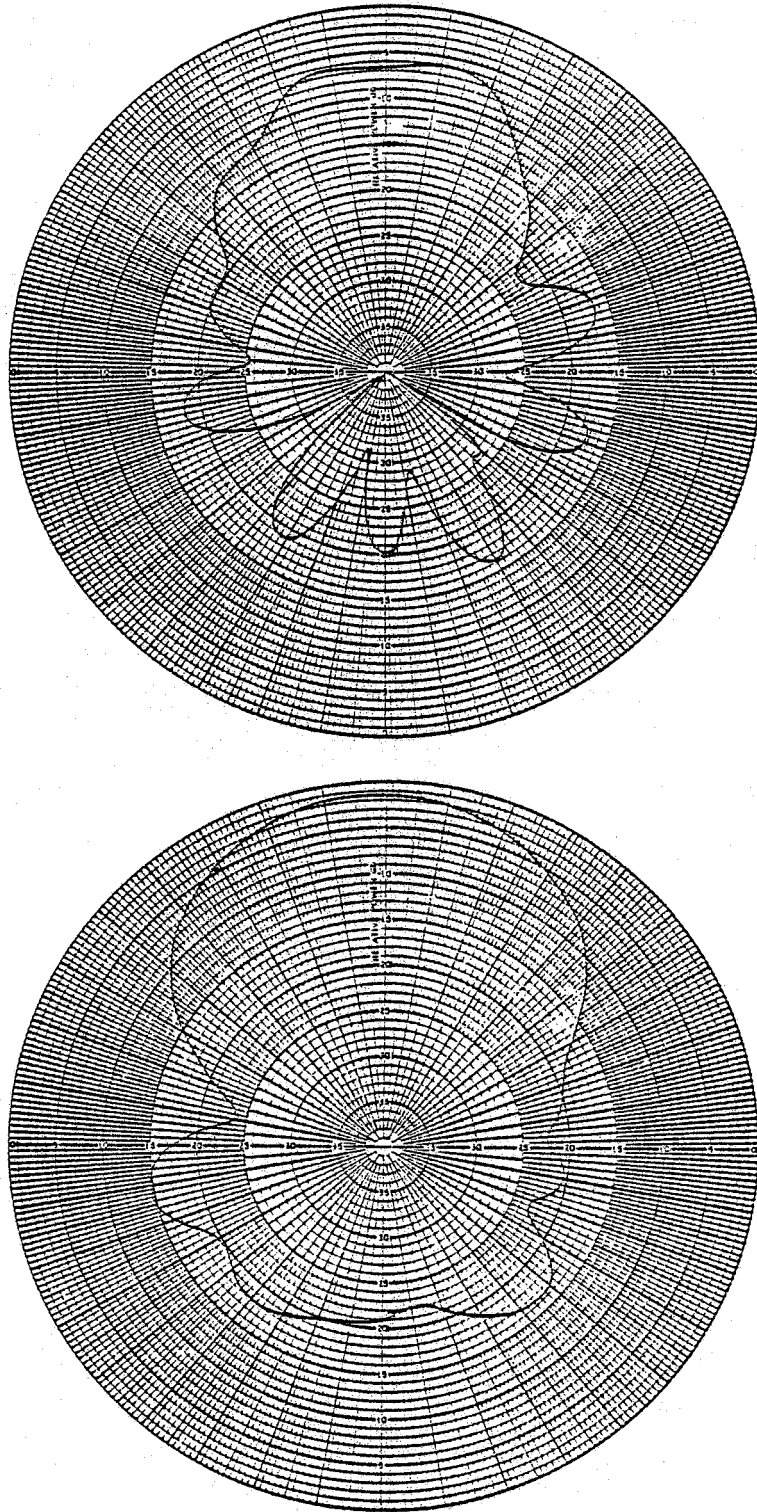


Fig. 12: Azimuthal (top) and elevation (bottom) plane patterns of the Radio Shack (VU60) receiving antenna at 527 MHz (Channel 23).

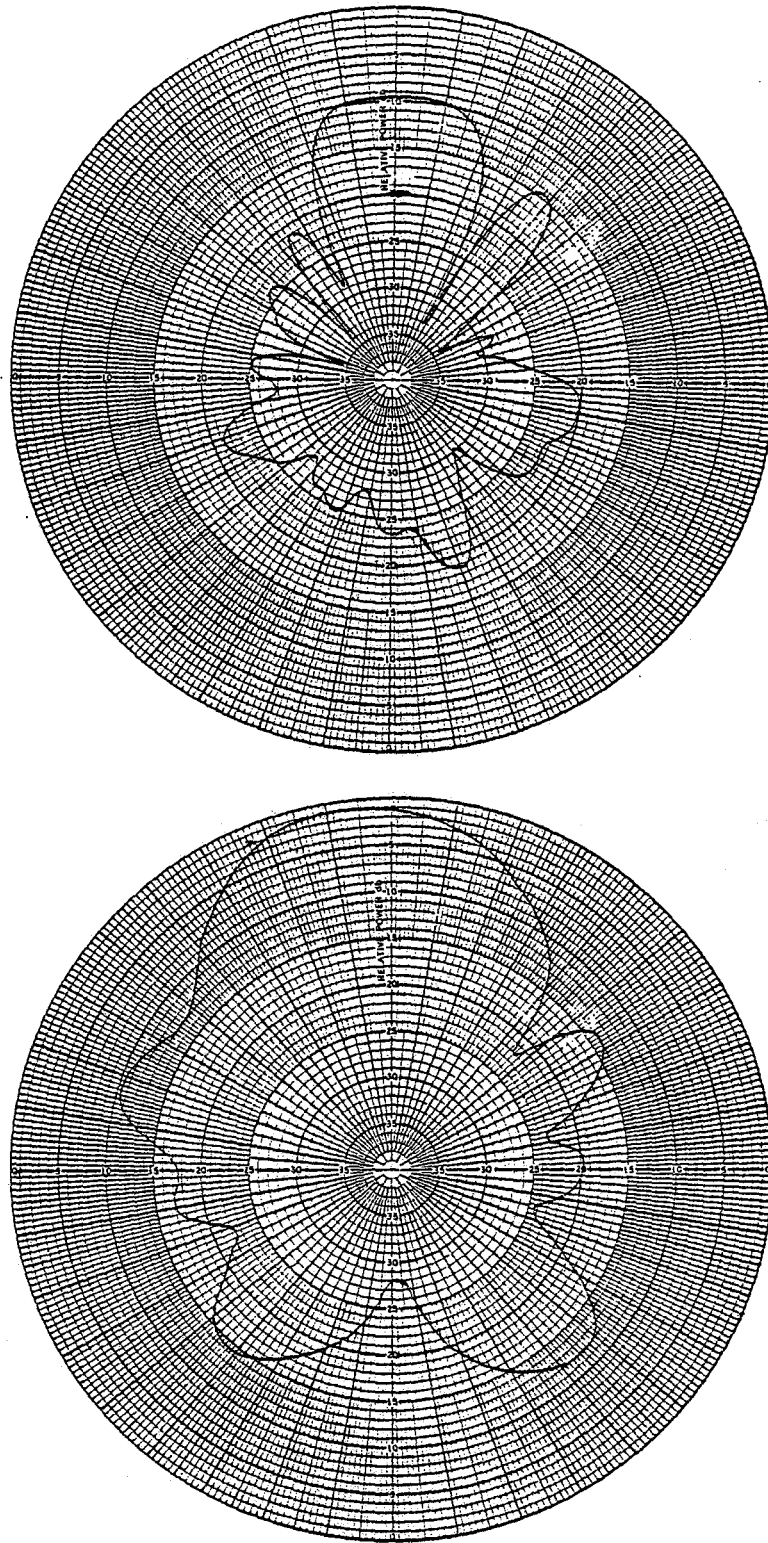


Fig. 13: Azimuthal (top) and elevation (bottom) plane patterns of the Radio Shack (VU60) receiving antenna at 677 MHz (Channel 48).

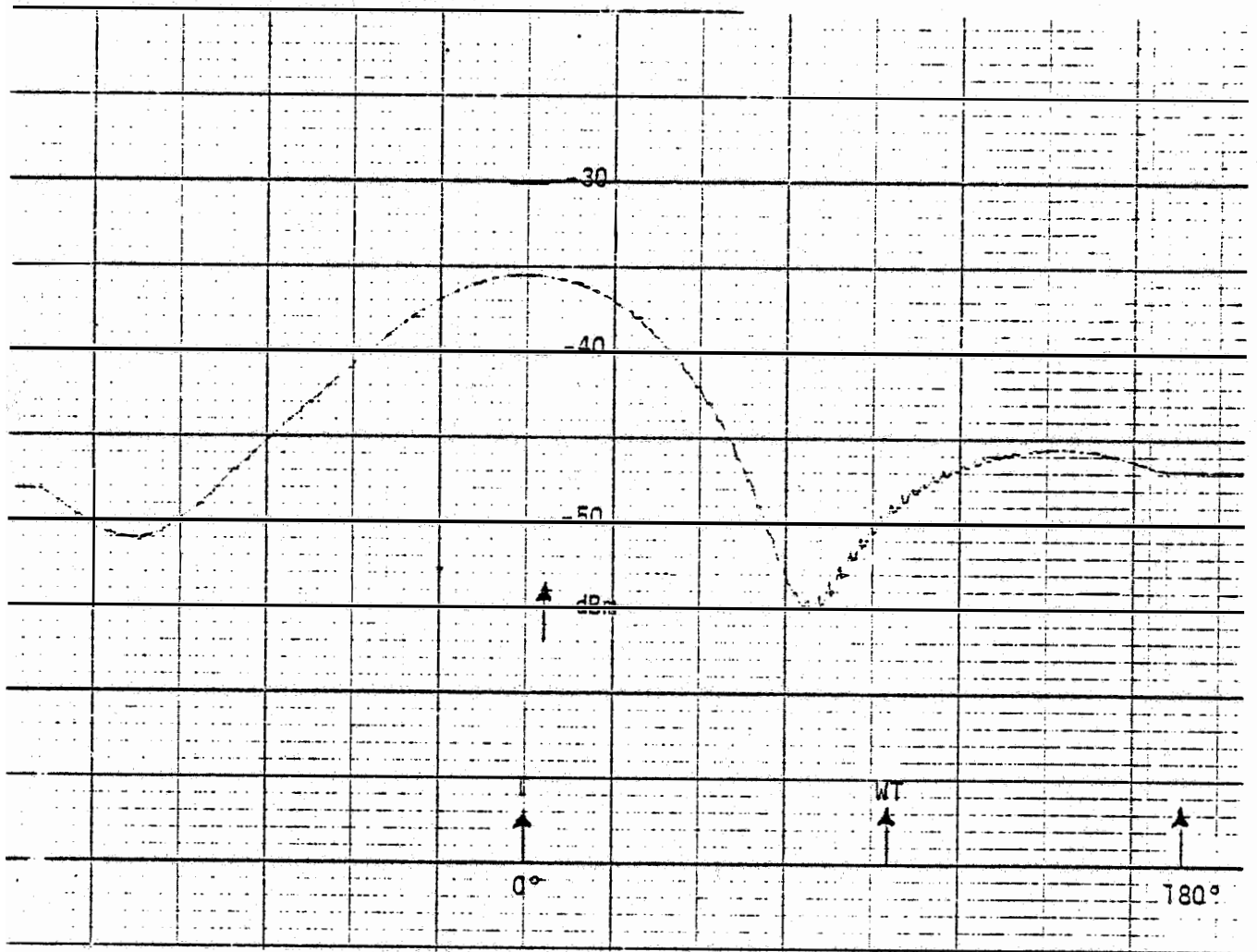


Fig. 14: Horizontal plane response of the test antenna on Channel 4 obtained at site 1.

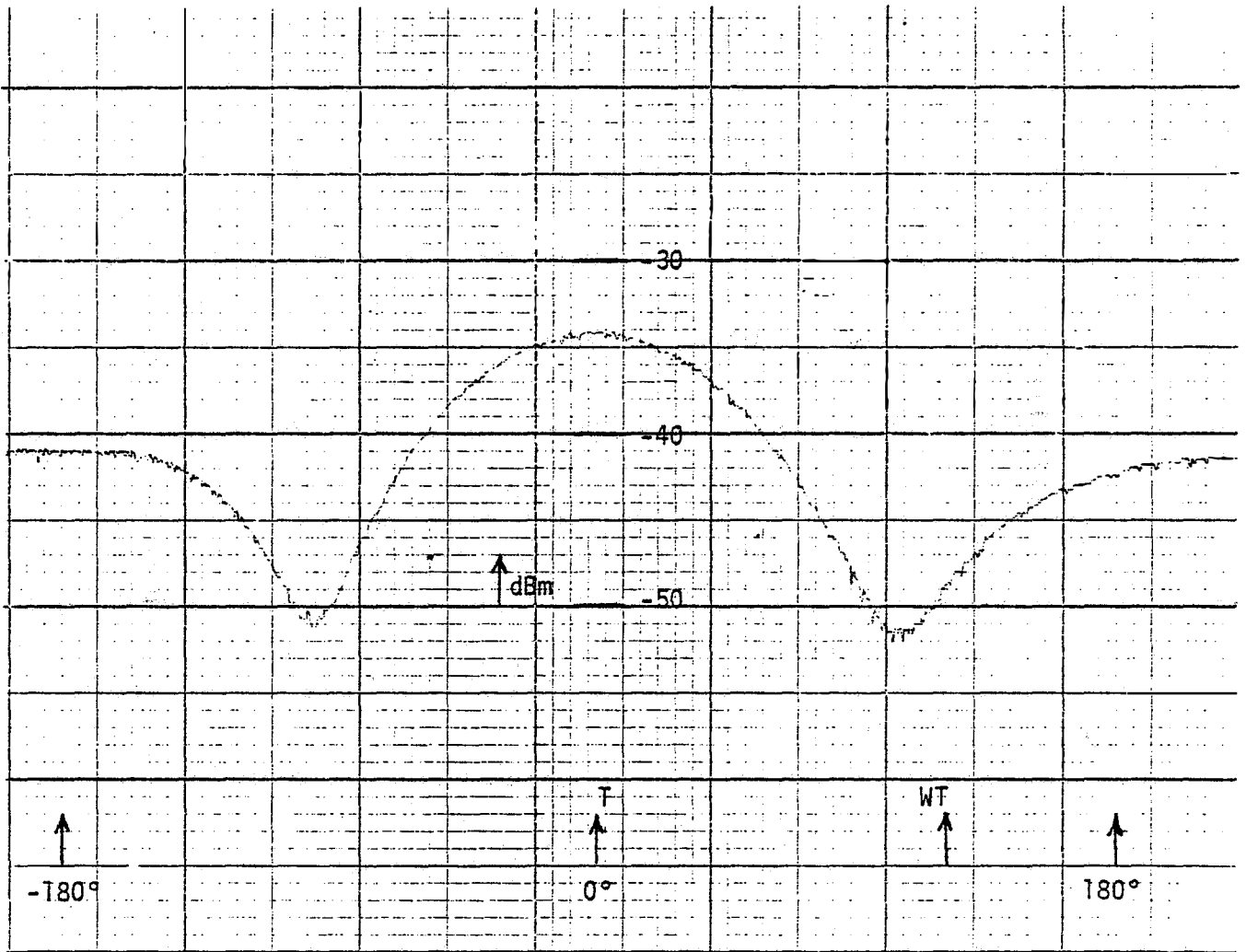


Fig. 15: Horizontal plane response of the test antenna on Channel 5 obtained at site 1.

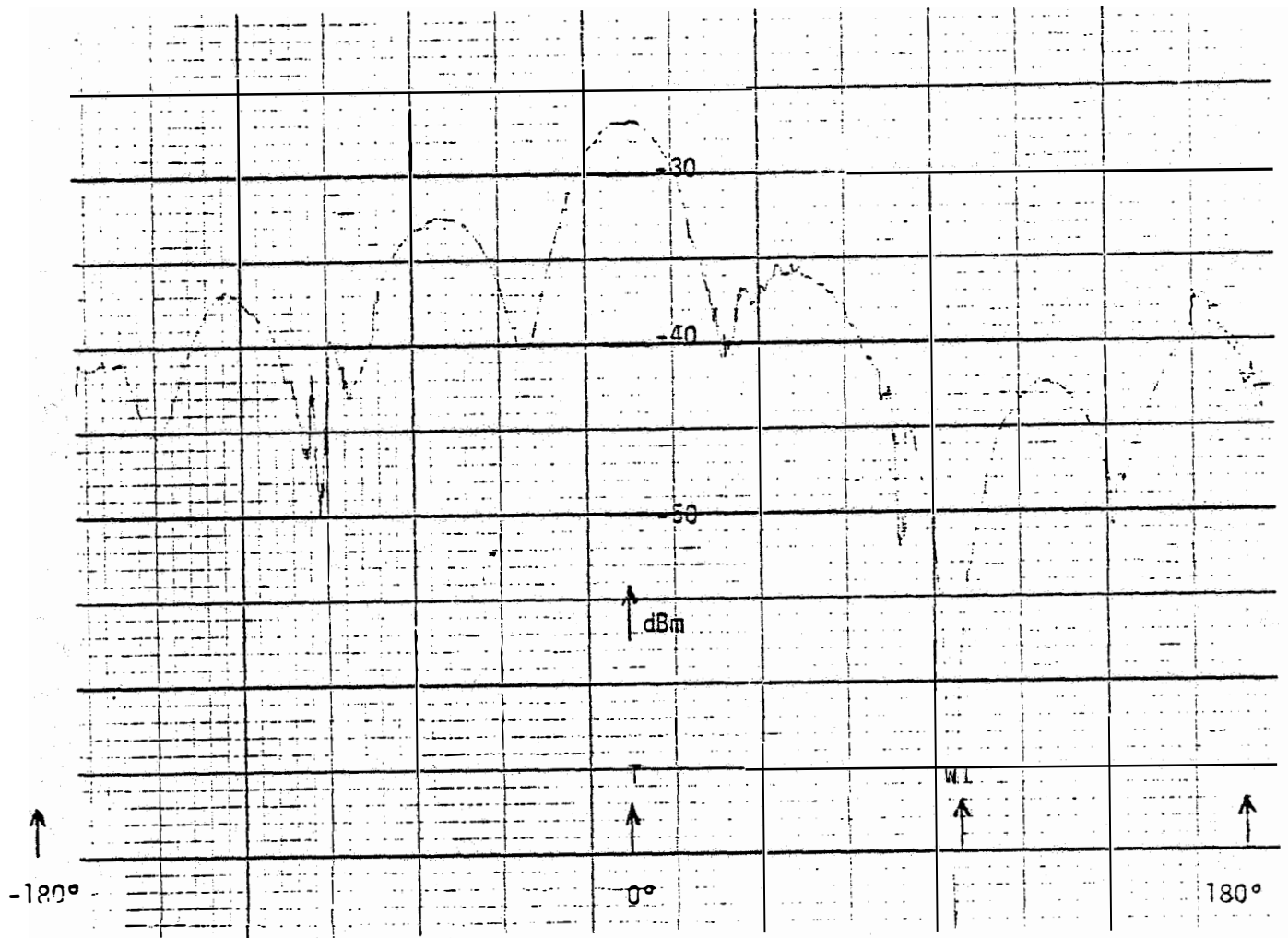


Fig. 16: Horizontal plane response of the test antenna on Channel 7 obtained at site 1.

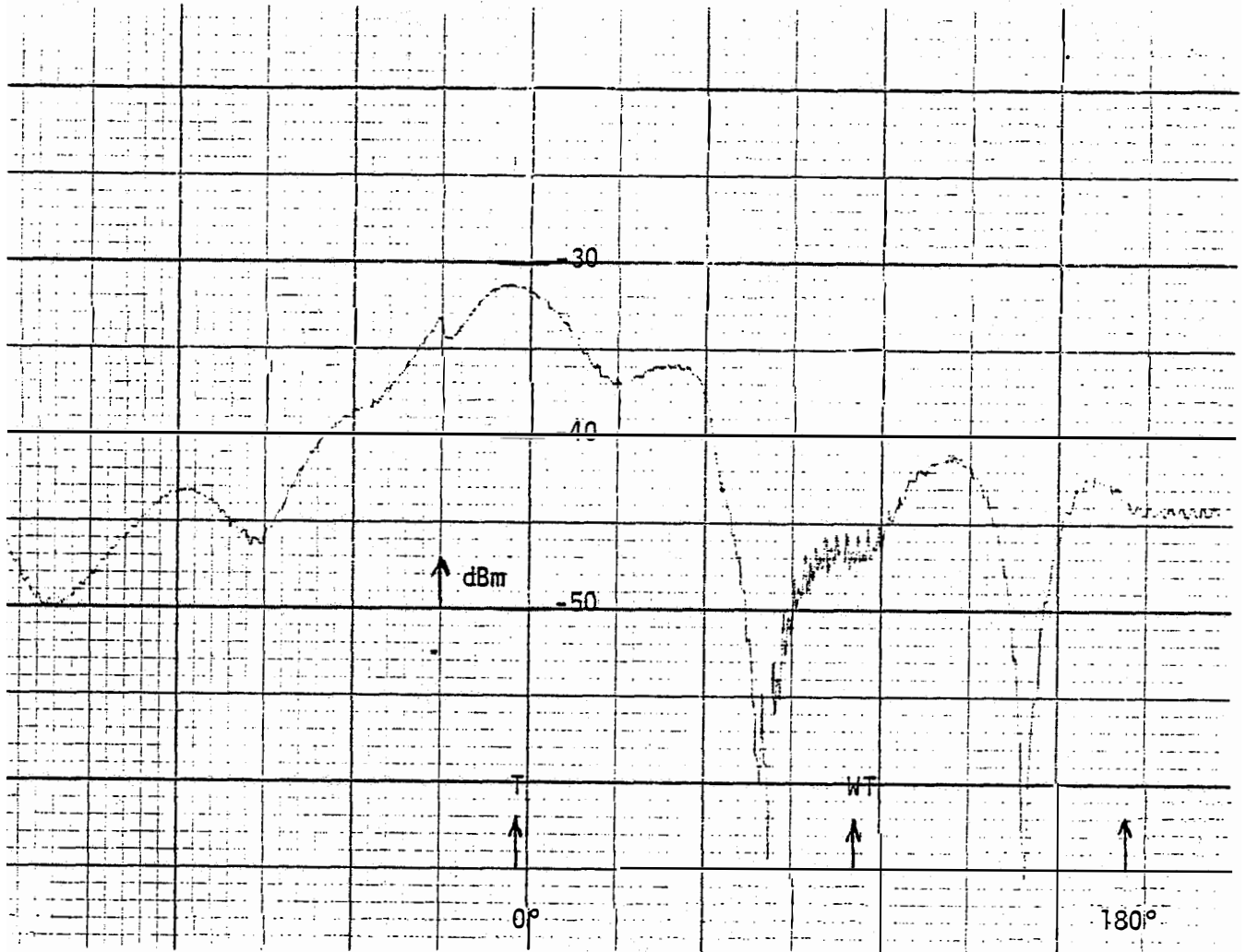


Fig. 17: Horizontal plane response of the test antenna on Channel 13 obtained at site 1.

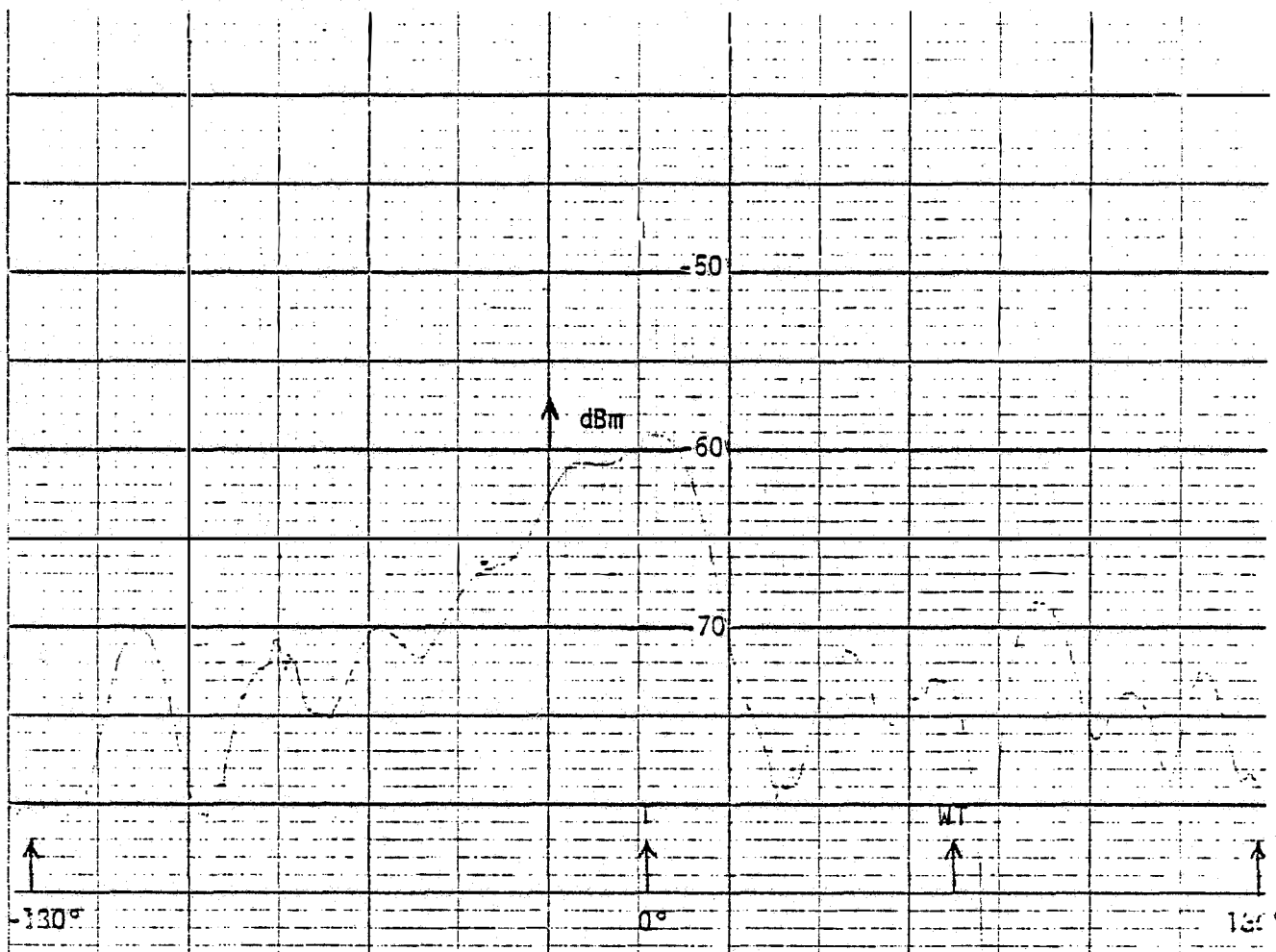


Fig. 18: Horizontal plane response of the test antenna on Channel 23 obtained at site 1.

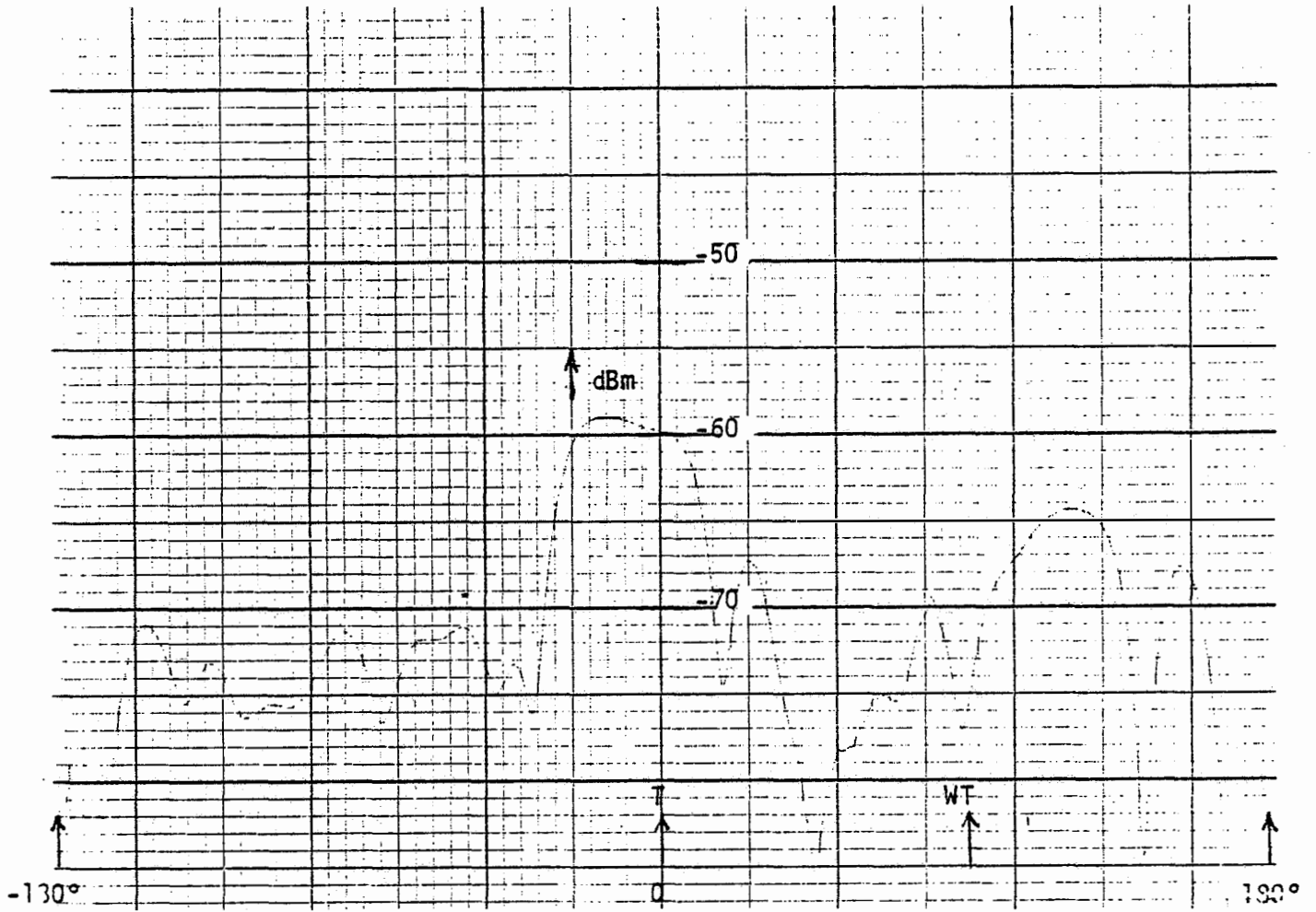


Fig. 19: Horizontal plane response of the test antenna on Channel 48 obtained at site 1.

3.3 Types of Measurement

At each test site, some or all of the following types of measurements were performed for every TV Channel of interest:

i) Received Signal Strength: With the WT stationary, the strength of the received signal was measured by rotating the main beam of the antenna until the output was a maximum. By tuning the spectrum analyzer through the TV Channel band of frequencies, a chart recording of the output versus frequency was obtained from which the video and audio signal strengths, P_v and P_a , respectively, in dBm (dB above one milliwatt) could be found.

ii) Antenna Response: As the antenna was rotated, the output P_a of the spectrum analyzer tuned to the audio carrier frequency was recorded as a function of time (and hence, the antenna position) with and without the WT operating. These measurements served to determine (a) the horizontal plane pattern of the antenna in the actual test environment, (b) the effect of the WT on the received signal and (c) the amount of signal modulation produced by the blade rotation.

iii) TV Interference: These dynamic tests were carried out with the VAWT operating at its normal speed, i.e., at 50.6 rpm. The antenna beam was positioned to receive the maximum audio signal (this generally occurred when the antenna beam was directed at the TV transmitter) and the spectrum analyzer was tuned to the audio carrier frequency of the desired signal. The output was then recorded as a function of time, and the received picture on the TV screen was also observed for any video distortion. In a few cases, the measurements were repeated with the antenna beam pointed at the WT to simulate the worst possible

situation of a mispositioned antenna. This generally provided a higher level of interference, and enabled us to see the modulation waveforms more clearly.

As mentioned earlier, the signal scattered by the rotating blades combines with the direct signal to produce an amplitude modulated signal at the inputs to the spectrum analyzer and the TV receiver. Thus, as a function of time, the output of the spectrum analyzer varies above and below the ambient level, and it is conventional to quote the total variation (Δ) of the received signal amplitude in dB from which the amplitude modulation index (m) can be obtained by using the relationship $\Delta = 20 \log_{10} (1+m)/(1-m)$. For future reference, the relationship between the percent modulation ($m \times 100$) and the total dB variation of the received signal is shown graphically in Fig. 20.

iii) Video Recording: This was done whenever it was felt desirable to preserve the video effects.

iv) Photograph of the Modulation Waveform: In one case (site 7, Channel 13), the modulation waveforms produced were photographed for later evaluation. This was done with the oscilloscope and camera combination shown in Fig. 5, and with the antenna beam directed at the operating WT.

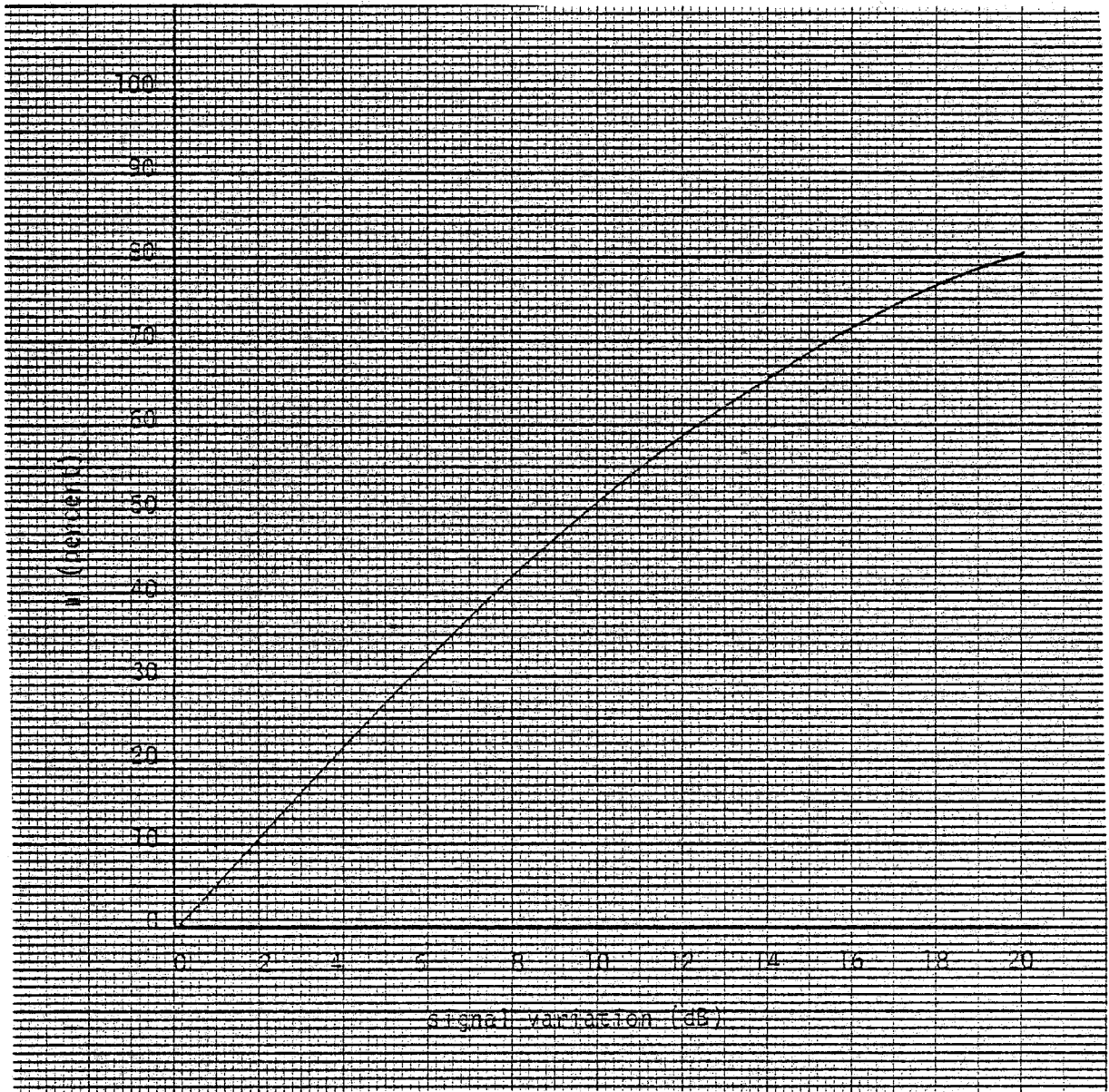


Fig. 20: Percent modulation as a function of the total dB variation of the observed signal.

CHAPTER 4. MEASURED AMBIENT FIELD STRENGTHS

To determine the quality of TV reception possible in the area, the ambient field strengths were measured at all of the test sites on all of the available TV Channels. There was also a second reason for the measurements. The severity of WT interference with TV reception depends on the ratio of the WT-scattered signal to the ambient signal at the site in question, and the WT-scattered signal is, in turn, proportional to the ambient field strength at the WT.

At each site and for all of the desired TV Channels, the received video and audio powers P_v and P_a , respectively, were obtained from the recordings of the spectrum analyzer output in the manner described in Section 3.3. In addition, the quality of reception was examined using the TV receiver. With the antenna oriented to receive the maximum signal, the spectrum analyzer was tuned through the TV Channel band of frequencies and the output recorded. Typical of the results obtained are those shown in Fig. 21 for Channel 4 at site 1. As true for all TV Channels, the audio power peak occurs at a frequency 4.5 MHz above the video power peak. The received video and audio carrier signal strengths can be obtained directly in dBm (dB above one milliwatt), and from Fig. 21 we have $P_v = -29$ dBm.

Recordings similar to these were made at all sites, and it is sufficient to present only the key quantities determined from them. P_v and P_a are of particular interest, and these are given in Tables 5 and 6, respectively.

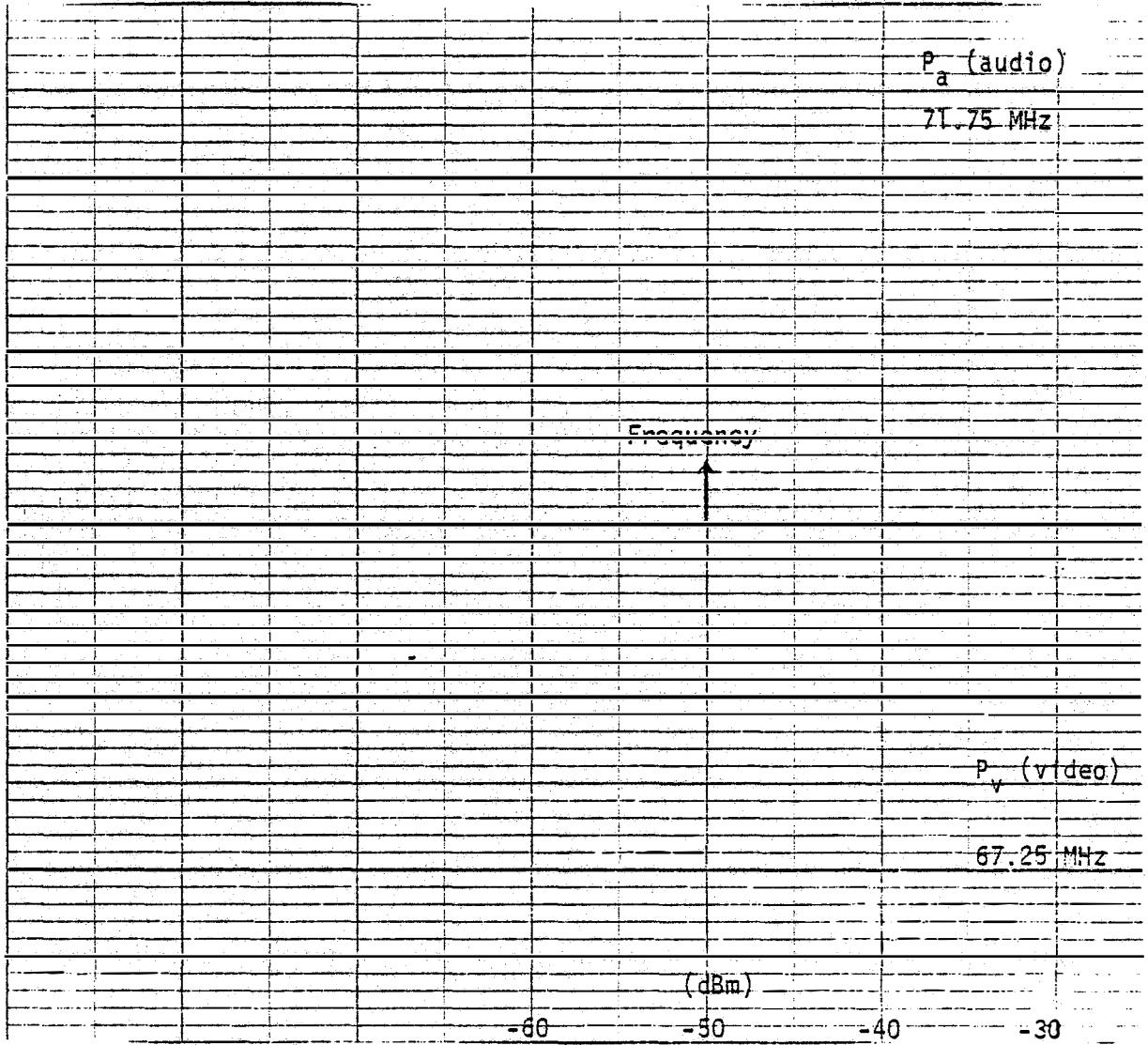


Fig. 21: Video and audio carrier signal strengths received on Channel 4 at site 1.

Table 5
Received Video Carrier Signal Strengths at the Test Sites

TV Channels	P_v (-dBm)							
	Test Sites							
	1	2	3	4	5	6	7	8
4	29	29	25	27	29	30	38	30
5	31	29	24	25	29	28	29	30
7	32	27	33	30	27	27	29	30
13	40	27	30	24	29	30	28	28
23	53	47	56	65	69	70	60	75
48	53	47	50	43	47	46	46	50

Table 6
Received Audio Carrier Signal Strengths at the Test Sites

TV Channels	P_a (-dBm)							
	Test Sites							
	1	2	3	4	5	6	7	8
4	36	36	32	33	36	38	35	36
5	34	35	30	32	36	36	34	34
7	31	27	30	26	30	28	30	26
13	36	31	37	31	32	34	33	30
23	59	65	70	71	75	76	69	82
48	59	56	60	52	57	56	54	54

The data in Tables 5 and 6 indicate that the VHF signals (Channels 4, 5, 7 and 13) were not significantly site-sensitive, although P_v was lower than P_a for Channel 7 at some sites, and for Channel 13 at site 1. No reason for this is known. The UHF signals (Channels 23 and 48) were typically 20 dB lower than the VHF ones, and did show some variation from site to site. The VHF Channel signals were quite strong at all sites and provided good quality TV reception. Channel 48, though weaker than the VHF Channels, was also strong enough to provide good reception except at sites 1 and 3 where the quality of reception was poor but acceptable. The Channel 23 signal was weakest of all, and its reception quality at the test sites varied from poor to unacceptable.

CHAPTER 5. DYNAMIC ANTENNA RESPONSE

This was measured by recording the audio signal carrier strength P_a as a function of the antenna beam pointing direction with the WT in operation. The results obtained at site 3 with the Darrieus rotating at 50.6 rpm (period \approx 1.2 sec) are shown in Figs. 22 through 27. The modulation pulses introduced by the blade rotation are clearly seen. The pulses occur every 0.6 sec (half the blade rotation period), and because the site is in the forward interference region (see Fig. 5), their amplitudes are independent of the antenna beam direction. As expected, the amplitudes increase with TV Channel frequency. On the VHF Channels the total signal variation Δ caused by the pulses varied from 0.5 to 1.5 dB, but was about 3 dB on Channels 23 and 48. In view of these levels it is not surprising that no significant video distortion was observed at VHF frequencies whereas on the UHF Channels the distortion was close to the threshold.

Site 2 was in the backscattering direction and the results obtained here are shown in Figs. 28 through 33. Because of the discrimination between the direct and WT-scattered signals which the antenna now provides, the amplitudes of the modulation pulses vary with the antenna beam pointing direction and are largest when the antenna is pointed at the WT. With the antenna properly oriented to receive the direct signal, there should be no video distortion on any of the six Channels at this site, and this was in fact the case.

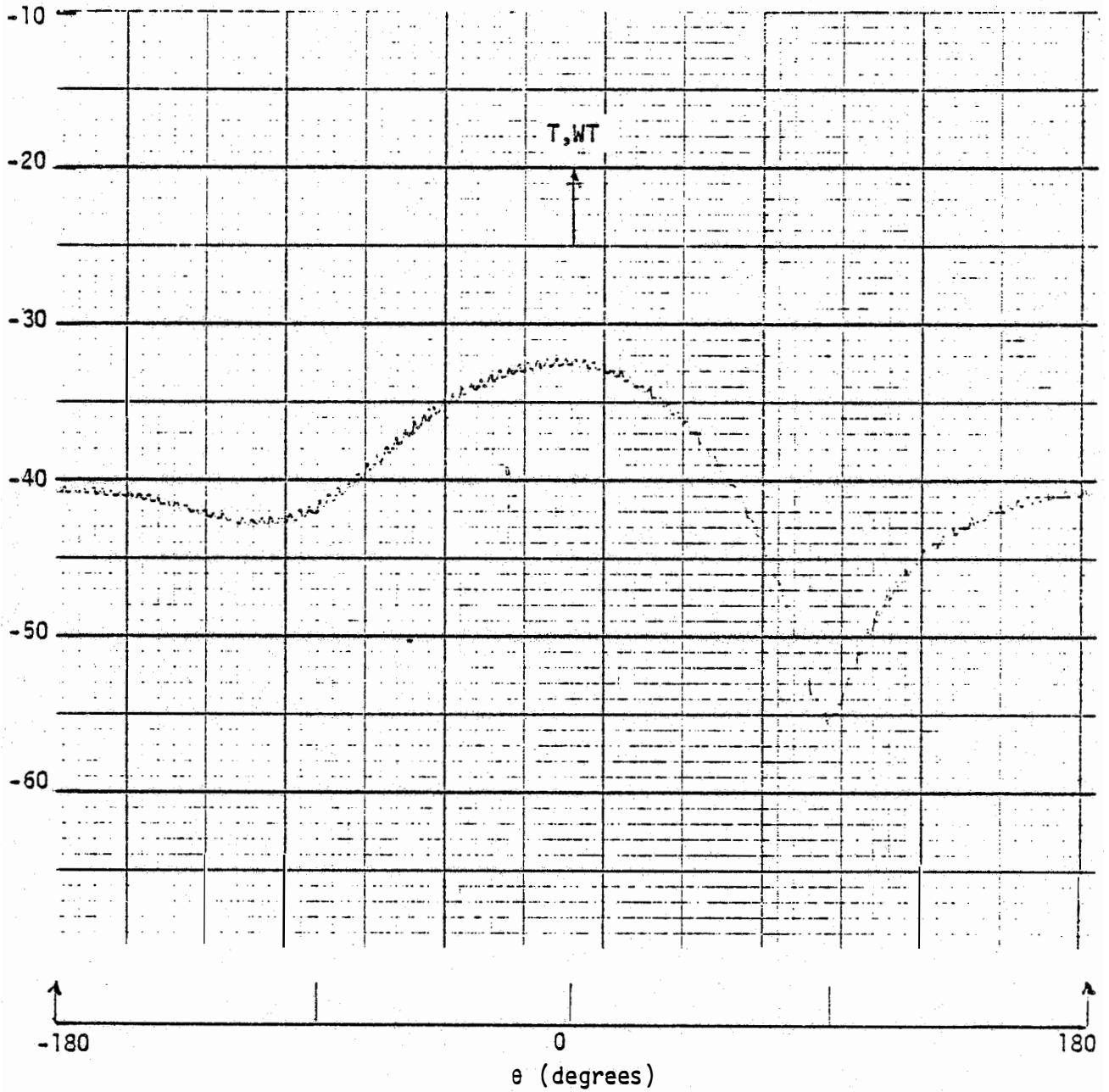


Fig. 22: Antenna response P_a (in dBm) as a function of the pointing direction at site 3, Channel 4.

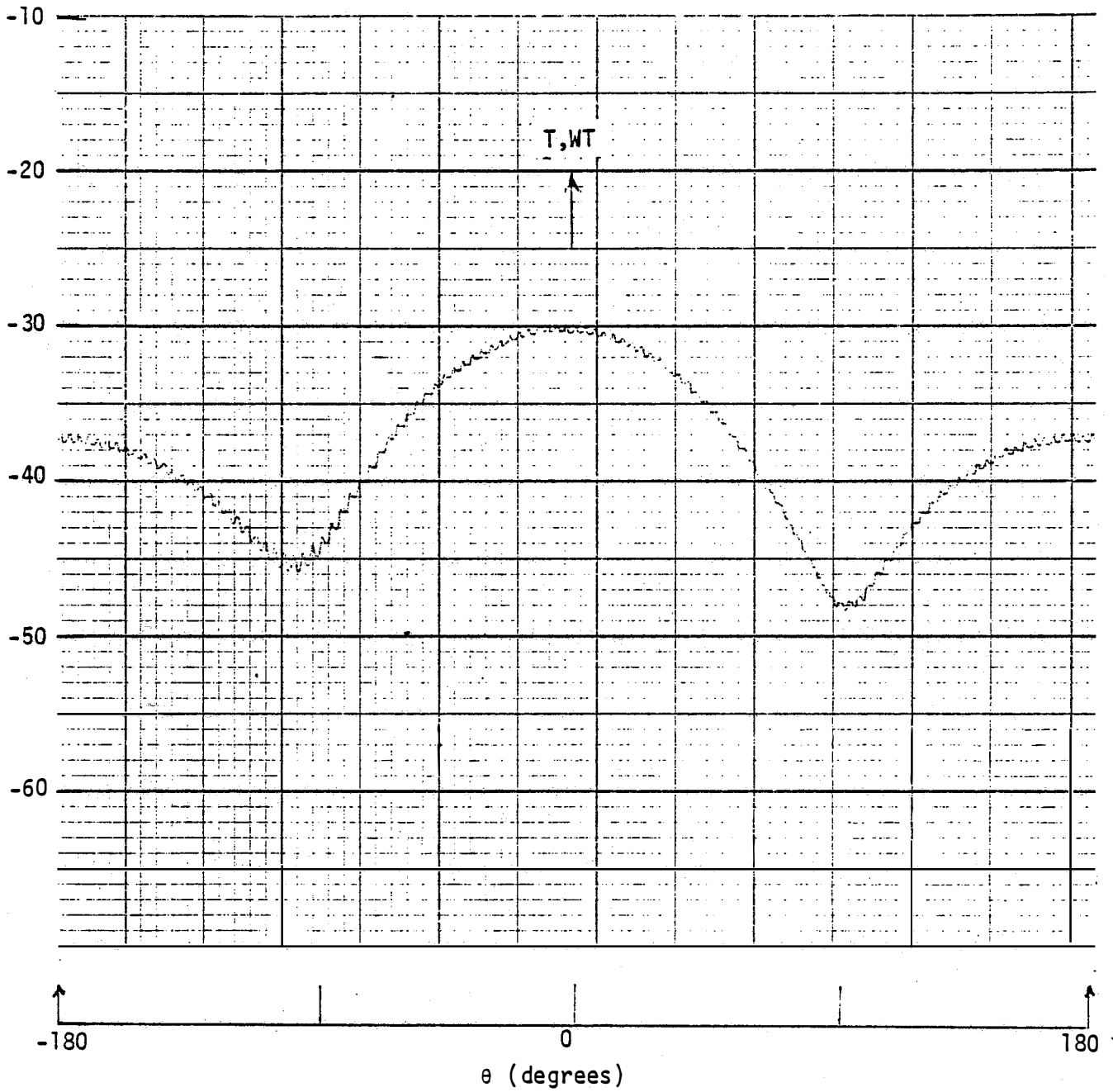


Fig. 23: Antenna response P_a (in dBm) as a function of the pointing direction at site 3, Channel 5.

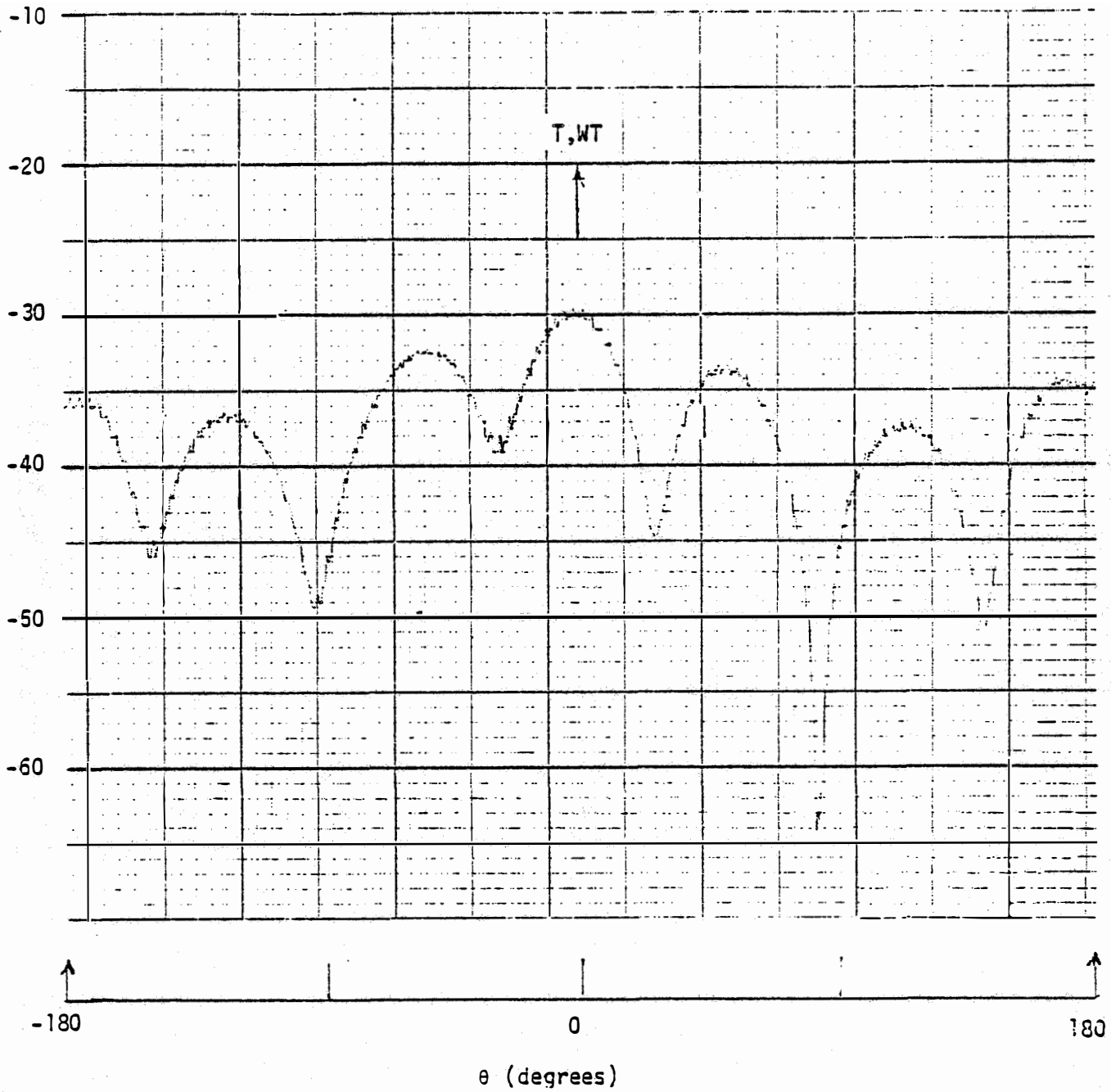


Fig. 24: Antenna response P_a (in dBm) as a function of the pointing direction at site 3, Channel 7.

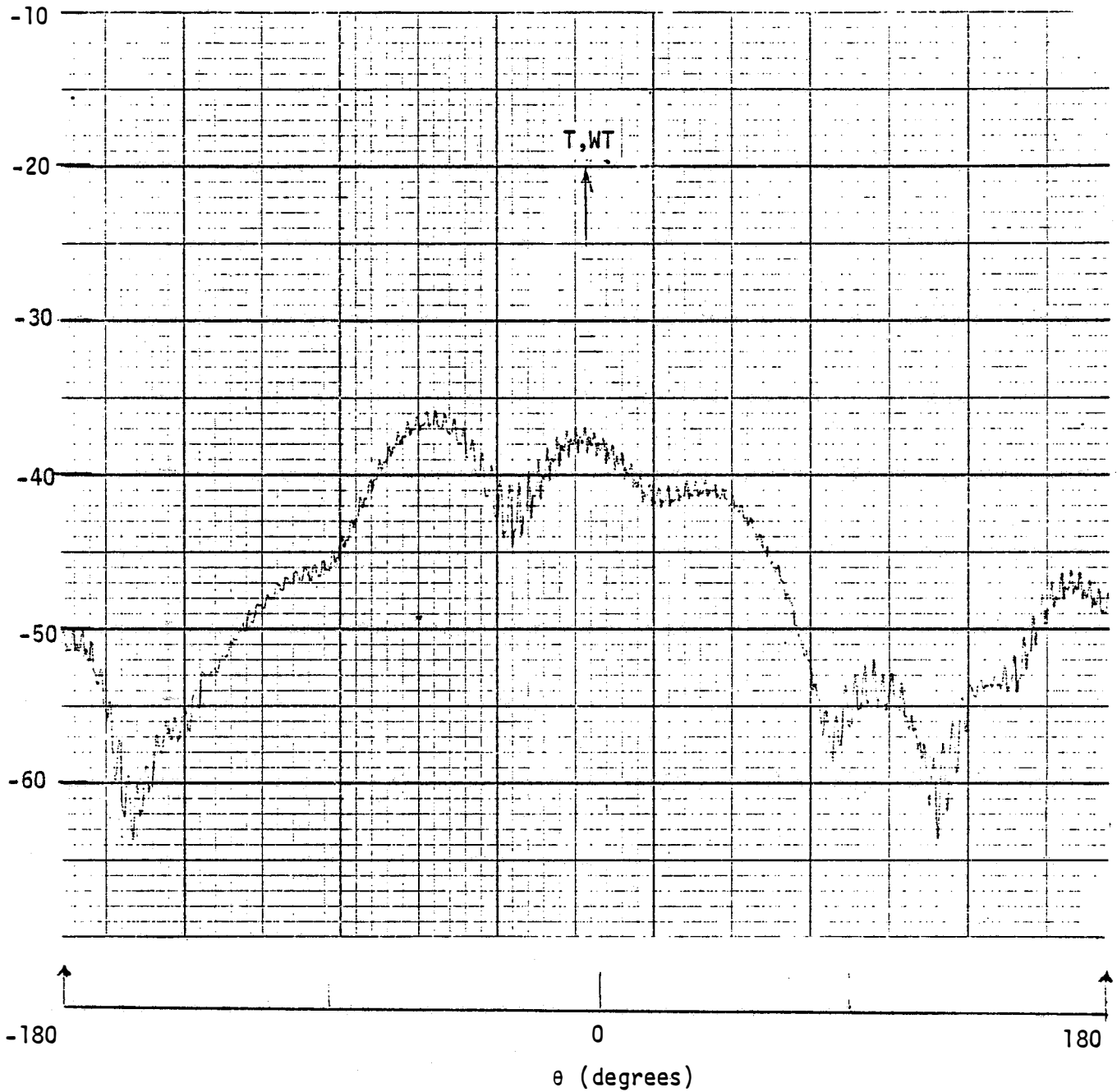


Fig. 25: Antenna response P_a (in dBm) as a function of the pointing direction at site 3, Channel 13.

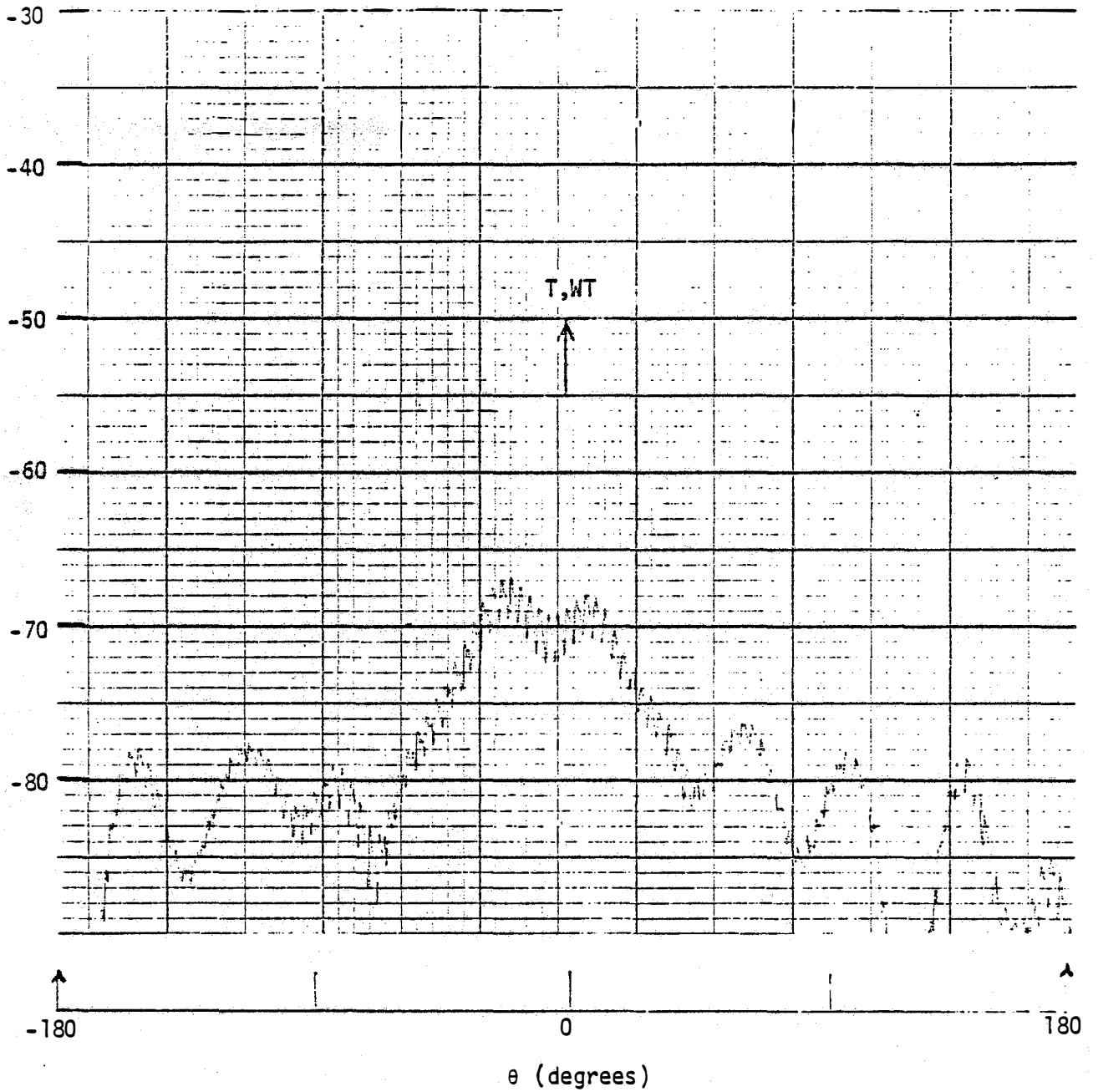


Fig. 26: Antenna response P_a (in dBm) as a function of the pointing direction at site 3, Channel 23.

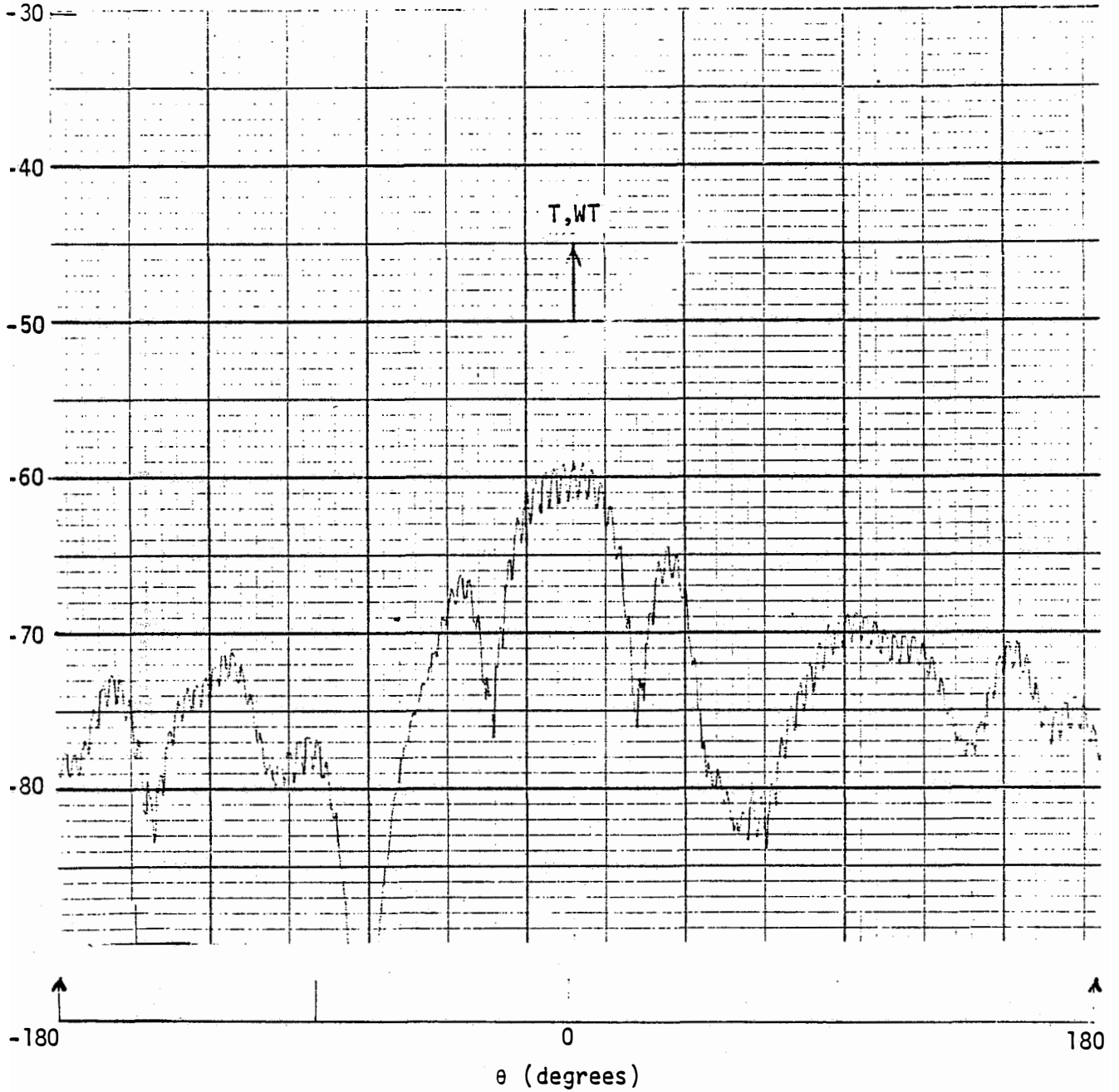


Fig. 27: Antenna response P_a (in dBm) as a function of the pointing direction at site 3, Channel 48.

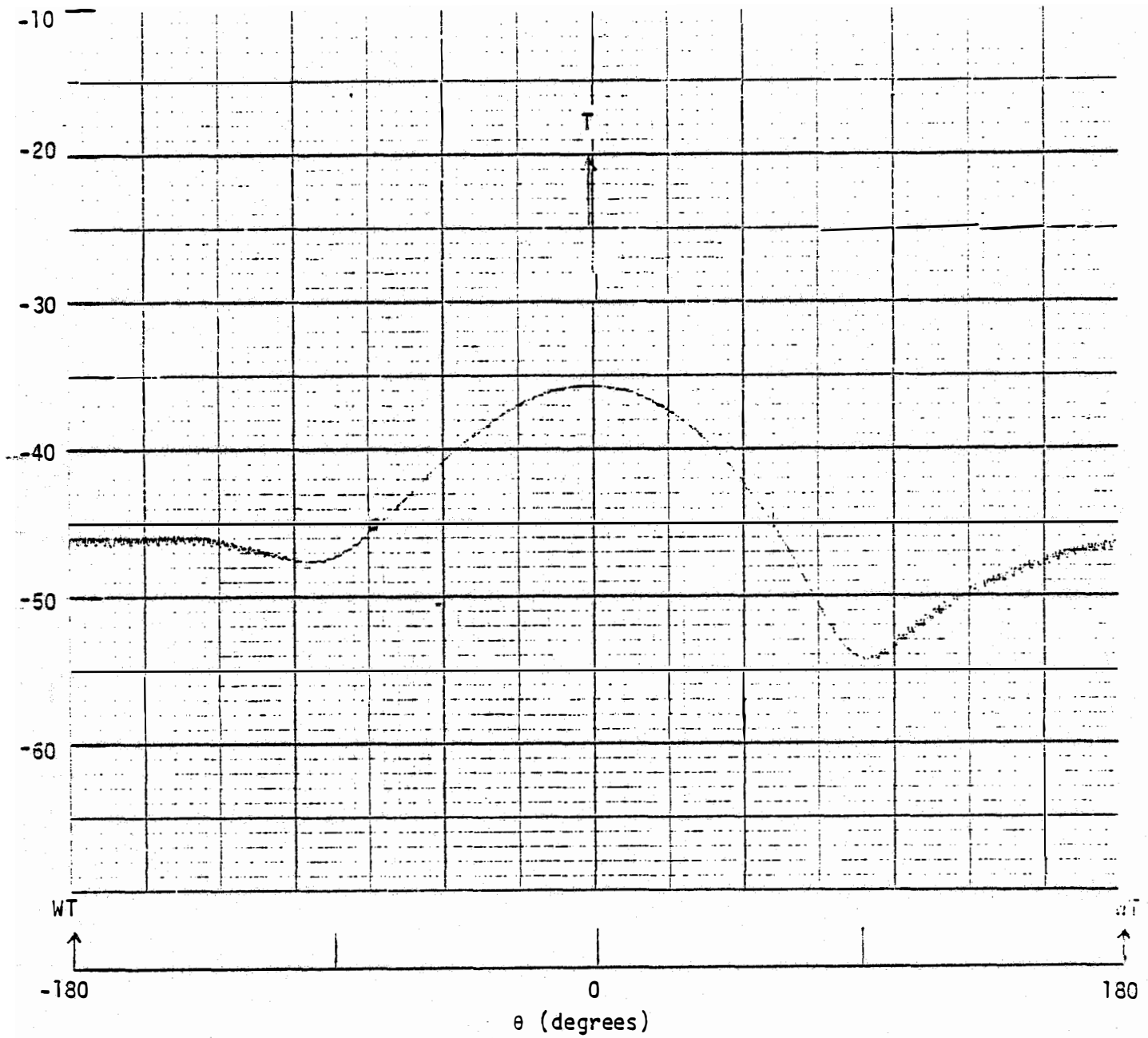


Fig. 28: Antenna response P_a (in dBm) as a function of the pointing direction at site 2, Channel 4.

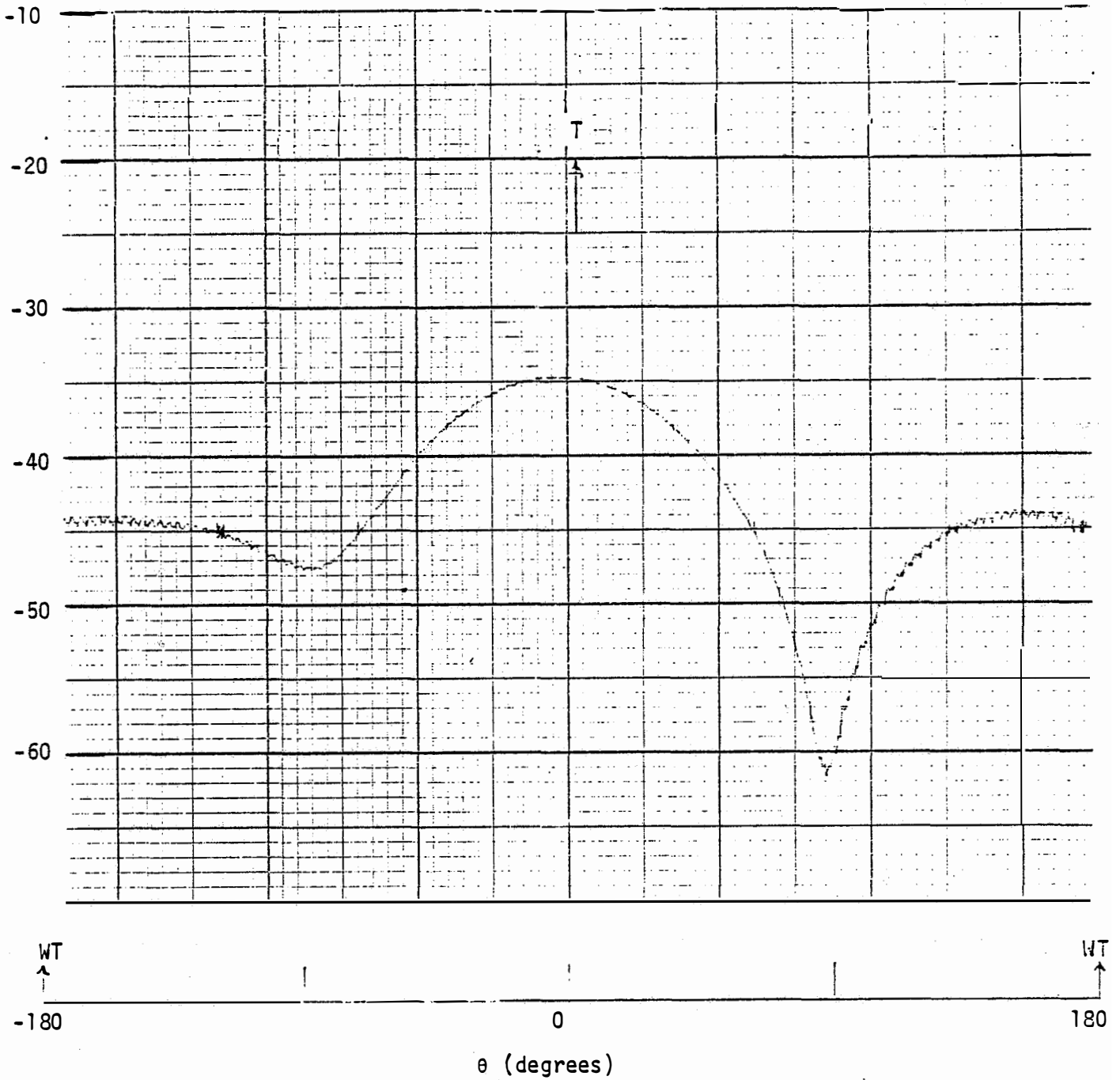


Fig. 29: Antenna response P_a (in dBm) as a function of the pointing direction at site 2, Channel 5.

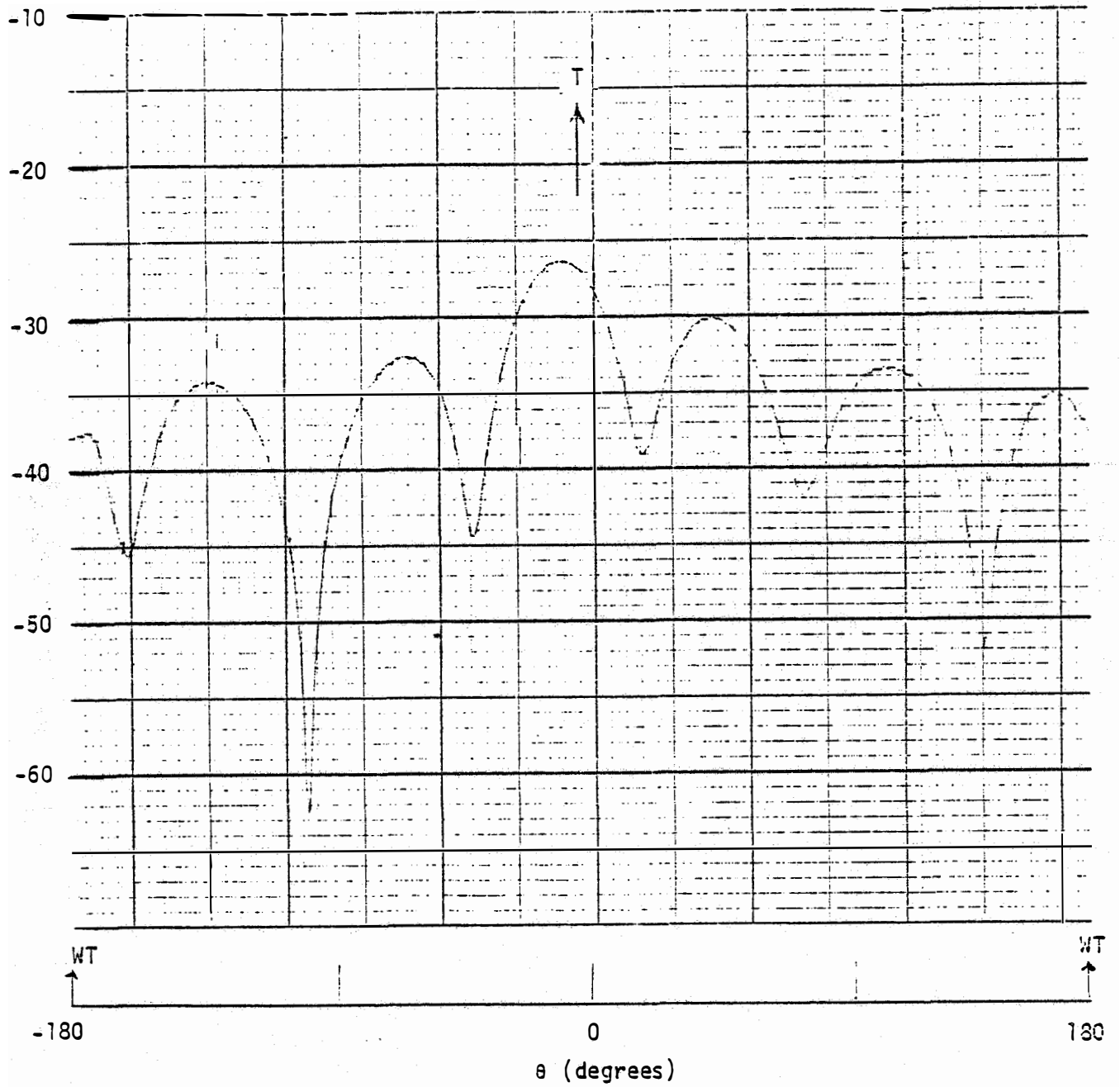


Fig. 30: Antenna response P_a (in dBm) as a function of the pointing direction at site 2, Channel 7.

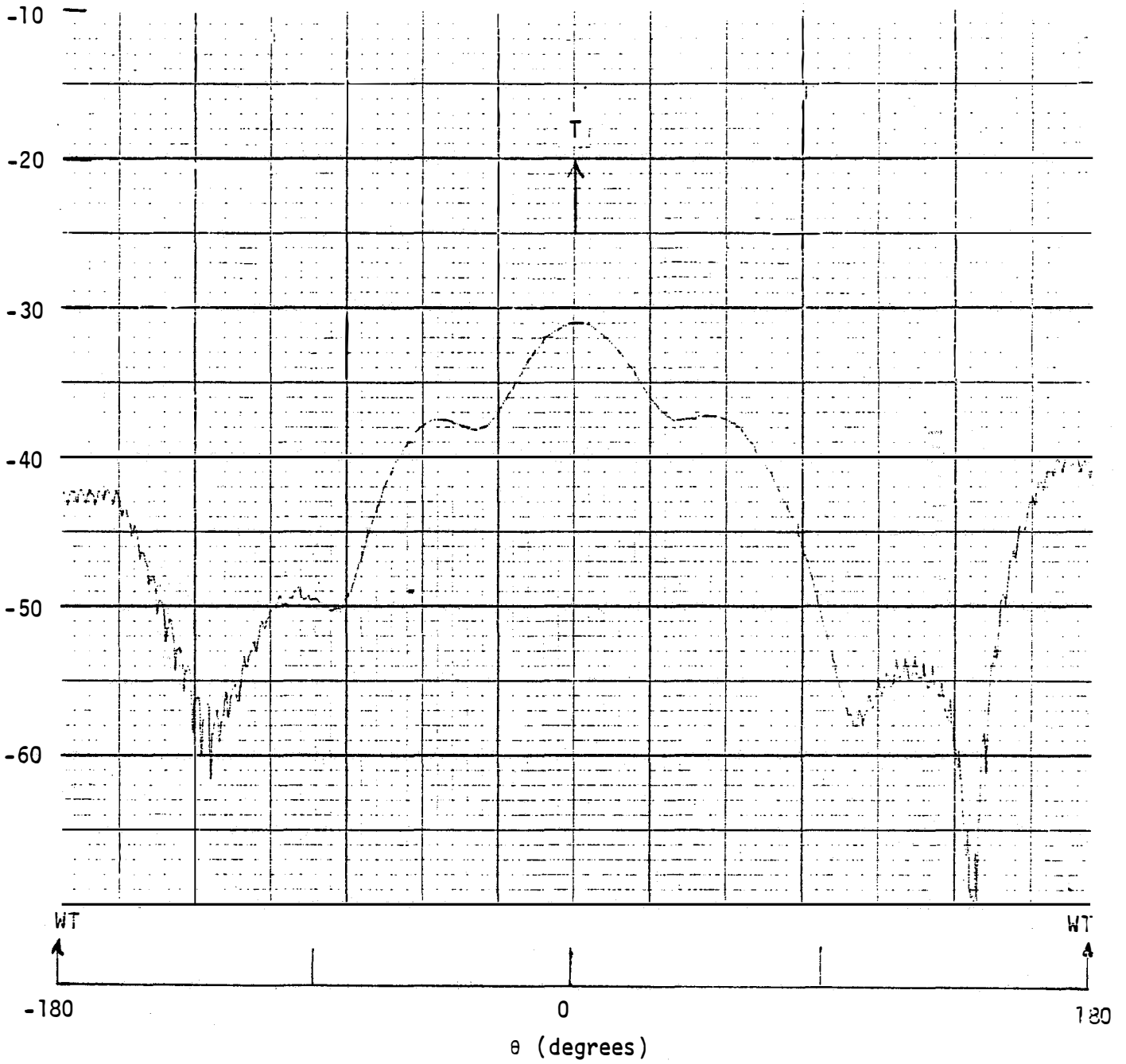


Fig. 31: Antenna response P_a (in dBm) as a function of the pointing direction at site 2, Channel 13.

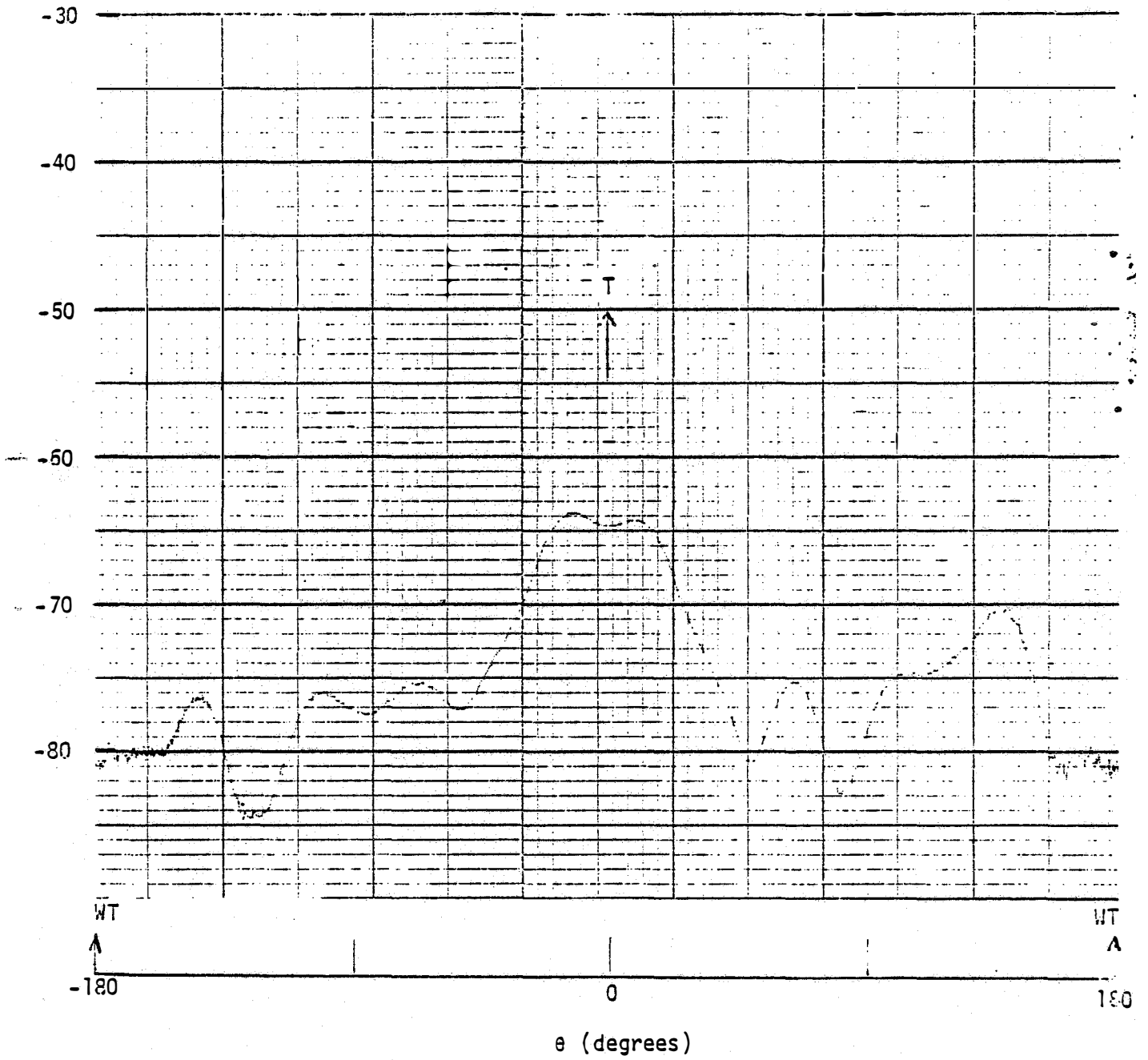


Fig. 32: Antenna response P_a (in dBm) as a function of the pointing direction at site 2, Channel 23.

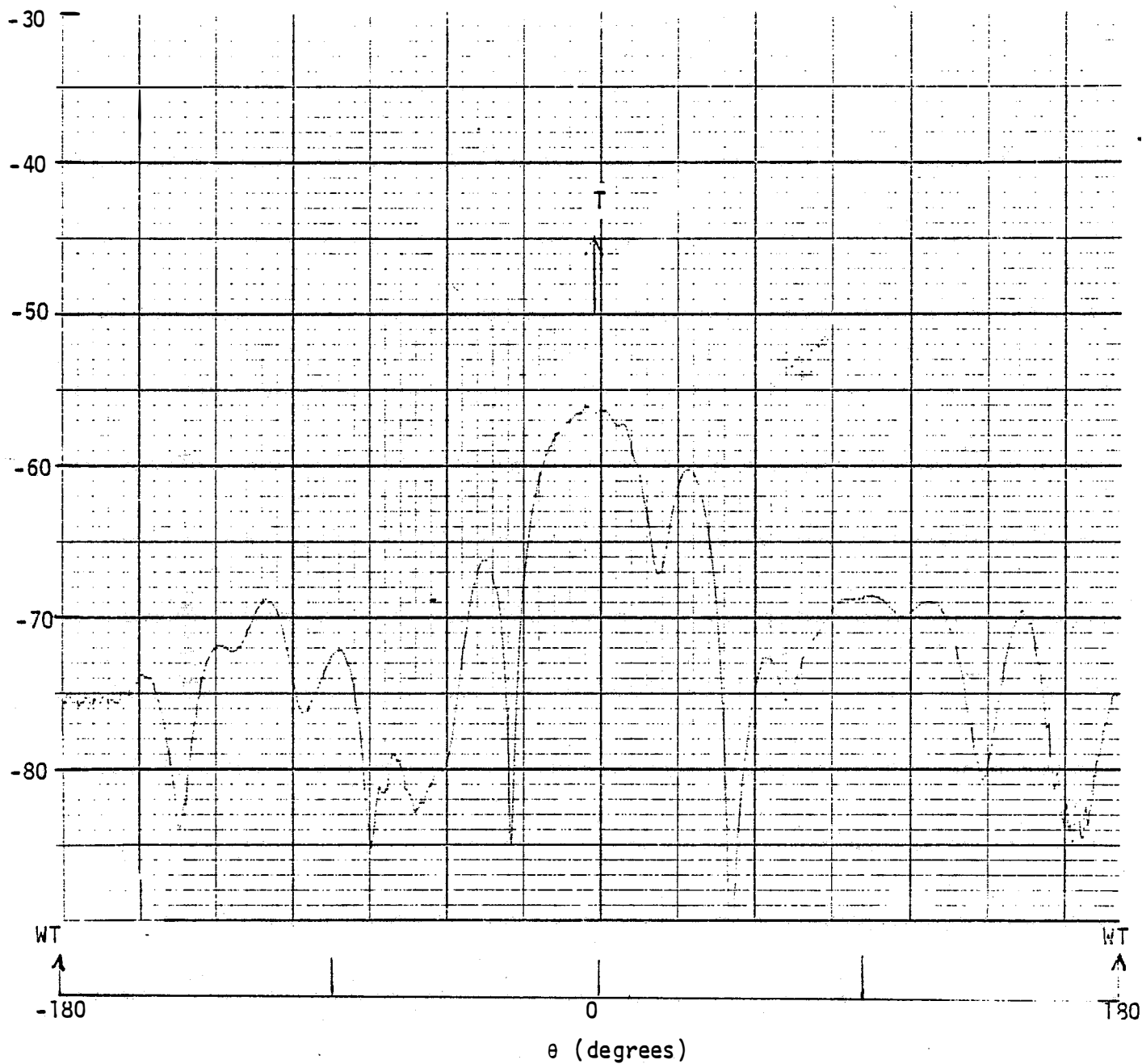


Fig. 33: Antenna response P_a (in dBm) as a function of the pointing direction at site 2, Channel 48.

Results similar to these were obtained at the other sites. By averaging out the modulation pulses, the smoothed versions of the antenna responses can be used to judge the horizontal plane patterns of the antenna in the test environment, and the dynamic data were used for this purpose as well as to investigate the interference. However, to study the TVI per se, more detailed measurements of the modulation pulses are required, and these are discussed in the next section.

CHAPTER 6. TELEVISION INTERFERENCE (TVI)

For a detailed examination of the interference produced by the operating Darrieus, recordings of P_a versus time were made at the various sites with the antenna beam pointed in an appropriate direction. At sites 3 and 5 in the forward interference region, the transmitter and the wind turbine were almost exactly in line, and the antenna was pointed at the transmitter/WT. The remaining sites were in the backward interference region and the antenna was then pointed successively at the transmitter (for optimum reception) and the WT (to enhance the interference effects). Throughout these measurements, the received picture was monitored for any video distortion.

6.1 Forward Region Interference

Portions of the recordings of P_a versus time at sites 3 and 5 are presented in Figs. 34 and 35 respectively, and the resulting values of the ambient field strength and total signal variation Δ attributable to the WT are listed in Table 7. Although the two sites are close together, the ambient field strengths differ from site to site on almost every Channel. This may be due to reflections from nearby objects.

All the VHF signals were quite strong at both sites and since $\Delta \leq 1.5$ dB it is not surprising that no video distortion was observed. At site 3 the Channel 48 signal was rather weak and there was some video distortion. There was no distortion at site 5, however, showing that a signal variation $\Delta \lesssim 1.5$ dB is too small to produce the

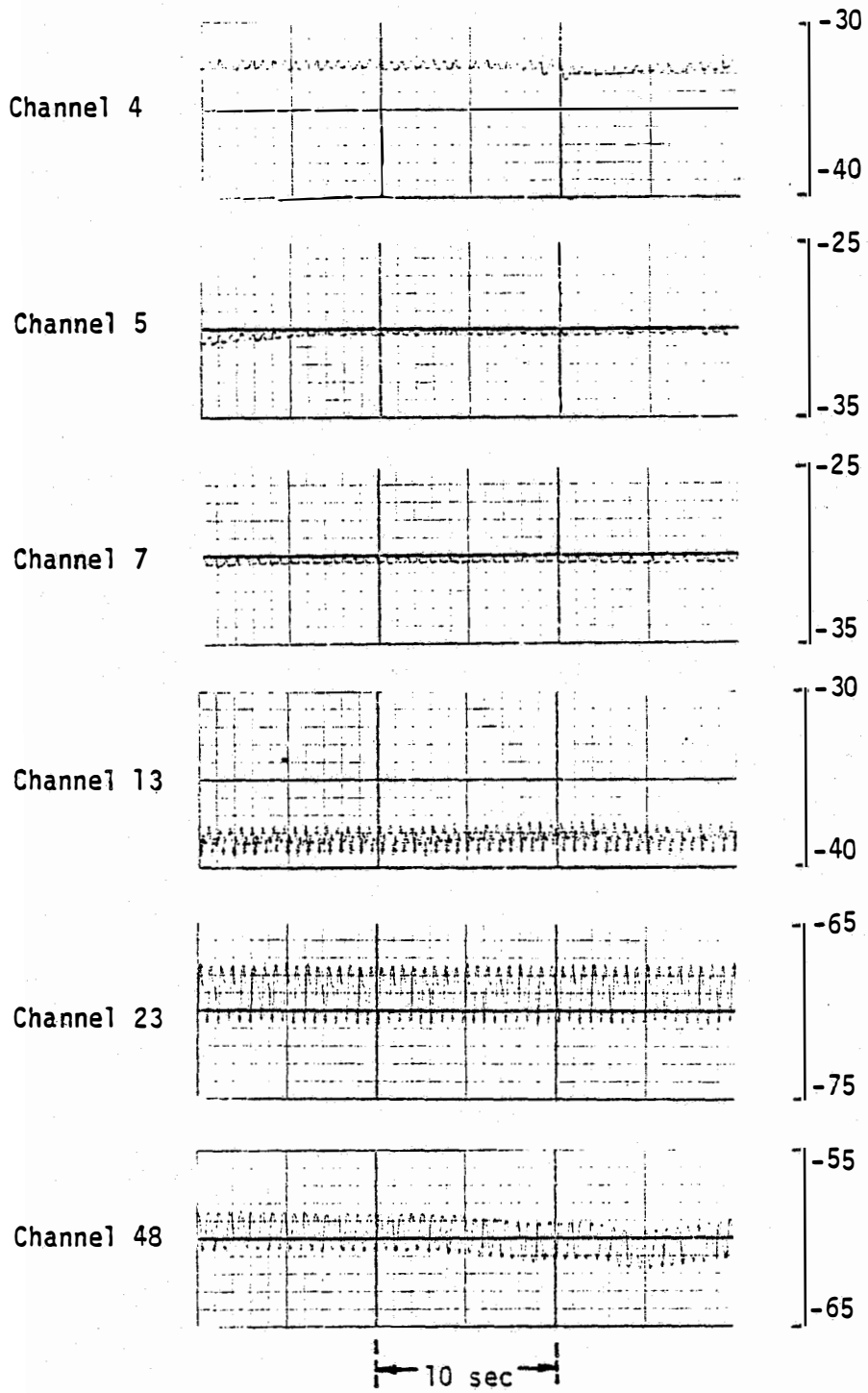


Fig. 34: P_a (in dBm) versus time at site 3.

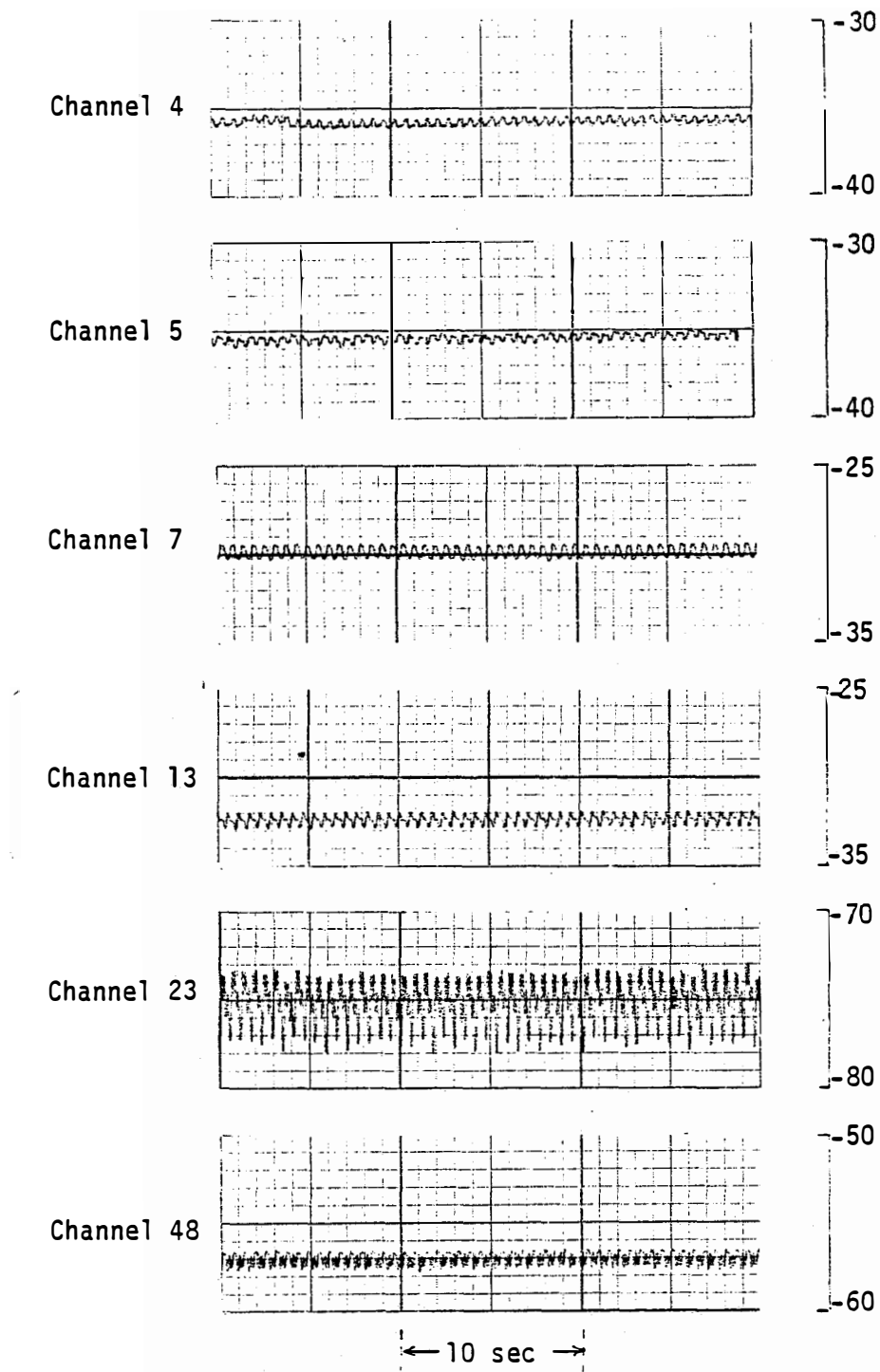


Fig. 35: P_a (in dBm) versus time at site 5.

Table 7

Received Ambient Field Strengths and Signal Variations
(caused by the Turbine Rotation) at Sites 3 and 5

TV Channel No.	Site 3		Site 5	
	Ambient P_a (-dBm)	Δ (dB)	Ambient P_a (-dBm)	Δ (dB)
4	32	1.0	36	0.6
5	30	0.5	36	1.0
7	30	0.7	30	1.0
13	38	1.5	32	1.0
23	69	4.0	75	5.0
48	- 60	2.5-3.0	57	1.5

forward region type of video distortion when the ambient signal strength is -57 dBm. The Channel 23 signals were much weaker, and the quality of reception was poor at site 3 and unacceptable at site 5. The signal variations were also larger than elsewhere. At site 3, $\Delta = 4$ dB and the video distortion was almost at the threshold level. At site 5, on the other hand, the distortion was quite unacceptable and well above the threshold level in spite of the fact that Δ was only 1 dB larger than at site 3. This clearly demonstrates that in the forward region the video distortion is a function of the ambient field strength as well as the total signal variation, with a weak signal being more vulnerable to distortion. Based on these results we conclude that in the forward interference region for a Darrieus the threshold level of Δ is approximately 4 dB, implying $m \approx 0.22$, for a signal level $P_a \approx -70$ dBm, but is higher for stronger fields and lower for weaker.

From the strip chart recordings of the modulation waveforms in Figs. 34 and 35 it is evident that the interference is periodic. It was observed that the interference and the resulting video distortion occurred whenever the 'loop' formed by the Darrieus blades was approximately in line with the receiver-transmitter direction, and this happens twice per rotation. However, the strip chart recorder has a relatively slow response and does not reveal the fine details of the waveform. When the output of the spectrum analyzer was observed, it was found that the waveform consists of broad pulses and narrow spikes and only the broad pulses appeared in Figs. 34 and 35. Consistent

with the findings in [3], the narrow spikes are larger in amplitude, and were we to have based the signal variations on these, the values of Δ would have been much larger, e.g., ≥ 10 dB on Channels 23 and 48. As judged by the relationship between Δ and the video distortion found [1-3] for a HAWT, the distortion observed with the Darrieus was nowhere near that associated with a total signal variation exceeding 10 dB, but was consistent with the values of Δ determined by the broad pulses. It would therefore appear that the narrow spikes seen in the output of the spectrum analyzer are not responsible for the observed distortion. This finding is consistent with the conclusions of our previous laboratory study [3] of VAWTs, and also carries over to backward region interference.

6.2 Backward Region Interference

Tests similar to those described above were conducted at the remaining six sites (1,3,4,6,7 and 8) located in the backward interference region. At each site recordings of P_a versus time were obtained with the antenna beam directed at the transmitter and at the WT. The former maximized the direct signal received, while the latter reduced the direct signal by the discrimination factor of the antenna, thereby enhancing the interference. The results are summarized in Tables 8 and 9 where the TVI effects are characterized by the following parameters:

- Q_i quality of video reception of grades $i = 0, 1, 2$ or 3 under normal conditions, i.e., with the WT stationary;
- D_i video distortion of grades $i = 0, 1, 2$ or 3 observed in the received picture.

The four grades of video reception and observed video distortion were established as follows:

video reception quality:

- Q_0 good
- Q_1 fair (little snowy)
- Q_2 poor (substantial snow)
- Q_3 very poor and unacceptable (extremely snowy)

observed video distortion:

- D_0 none or barely visible
- D_1 visible but below threshold
- D_2 comparable to the threshold
- D_3 above threshold/unacceptable.

In general, the four grades of video reception were in accordance with received ambient field levels in the following ranges:

- Q_0 $P_a \geq -56$ dBm
- Q_1 -56 dBm $> P_a \geq -65$ dBm
- Q_2 -65 dBm $> P_a \geq -70$ dBm
- Q_3 -70 dBm $> P_a$

and the four grades of video distortion corresponded approximately to a total signal variation Δ as follows:

- D_0 0.0 dB $\leq \Delta < 0.5$ dB
- D_1 0.5 dB $\leq \Delta < 2.5$ dB
- D_2 2.5 dB $\leq \Delta \leq 3.0$ dB
- D_3 $\Delta > 3.0$ dB.

We note that the threshold range is consistent with the previously established value $\Delta_0 = 2.6$ dB for the backward region, discussed in Sections 2.4 and 3.3.

The data in Table 8 show that with the antenna properly oriented to receive the maximum desired signal, the only video distortion observed was on Channel 23 at sites 6 and 8, whereas with the antenna beam directed at the WT (Table 9) there was distortion varying from acceptable to unacceptable on all Channels at all sites. It was observed that the distortion generally occurred when the plane formed by the blades bisected the angle between the WT-transmitter and WT-receiver directions, corresponding to the case of specular reflection off the blades.

It may be helpful to present some of the recordings of P_a versus time that were made with the antenna beam pointed at the WT. The results for site 2 are shown in Fig. 36. Barely visible amounts of distortion were seen on all Channels, the largest being on Channel 48 for which $\Delta \approx 1.5$ dB. Since site 2 was in the backscattering direction, the antenna served to discriminate against the direct signal as indicated by the dynamic antenna responses in Figs. 28 through 33, and this explains the differing amounts of video distortion in Tables 8 and 9.

Sites 6, 4 and 1 were located at increasing distances from the WT on the 90° radial approximately. At sites 6 and 4 varying degrees of video distortion were observed on all Channels, and the data are presented in Figs. 37 and 38 respectively. Under similar conditions no significant distortion was observed at site 1 on any Channel, though it is pertinent to remark that visible (slight) distortion was seen on Channel 4 ($\Delta \approx 1.0$ dB) for $P_a \approx -50$ dBm and on Channel 48 ($\Delta \approx 1.5$ dB) when the ambient field strength was $P_a \approx -73$ dBm.

Sites 7 and 8 are also comparable in being located on the 45° and 135° radials respective, and the data for these sites are shown in Figs. 39 and 40. At site 7 the low signal levels on

Table 8

Summary of Backward Interference Region TVI Data:

Antenna Beam Directed at the Transmitter, with WT Running at 50.6 rpm

TV Channel Number	TVI Parameters					
	Site 1	Site 2	Site 4	Site 6	Site 7	Site 8
4	Q ₀ D ₀					
5	Q ₀ D ₀					
7	Q ₀ D ₀					
13	Q ₀ D ₀					
23	Q ₁ D ₀	Q ₁ D ₀	Q ₃ D ₀	Q ₃ D ₃	Q ₂ D ₀	Q ₃ D ₃
48	Q ₁ D ₀	Q ₀ D ₀	Q ₀ D ₀	Q ₁ D ₀	Q ₀ D ₀	Q ₀ D ₀

Table 9

Summary of Backward Interference Region TVI Data:
 Antenna Beam Directed at the WT, Running at 50.6 rpm

TV Channel Number	TVI Parameters					
	Site 1	Site 2	Site 4	Site 6	Site 7	Site 8
4	Q ₀ D ₁	Q ₀ D ₁	Q ₀ D ₃	Q ₀ D ₂	Q ₀ D ₁	Q ₀ D ₁
5	Q ₀ D ₁	Q ₀ D ₁	Q ₀ D ₁	Q ₀ D ₃	Q ₀ D ₁	Q ₀ D ₁
7	Q ₀ D ₀	Q ₀ D ₁				
13	Q ₀ D ₀	Q ₀ D ₁	Q ₀ D ₁	Q ₀ D ₁	Q ₀ D ₃	Q ₀ D ₁
23	Q ₃ D ₁	Q ₃ D ₁	Q ₃ D ₃			
48	Q ₃ D ₁	Q ₃ D ₂	Q ₁ D ₂	Q ₃ D ₂	Q ₃ D ₂	Q ₃ D ₂

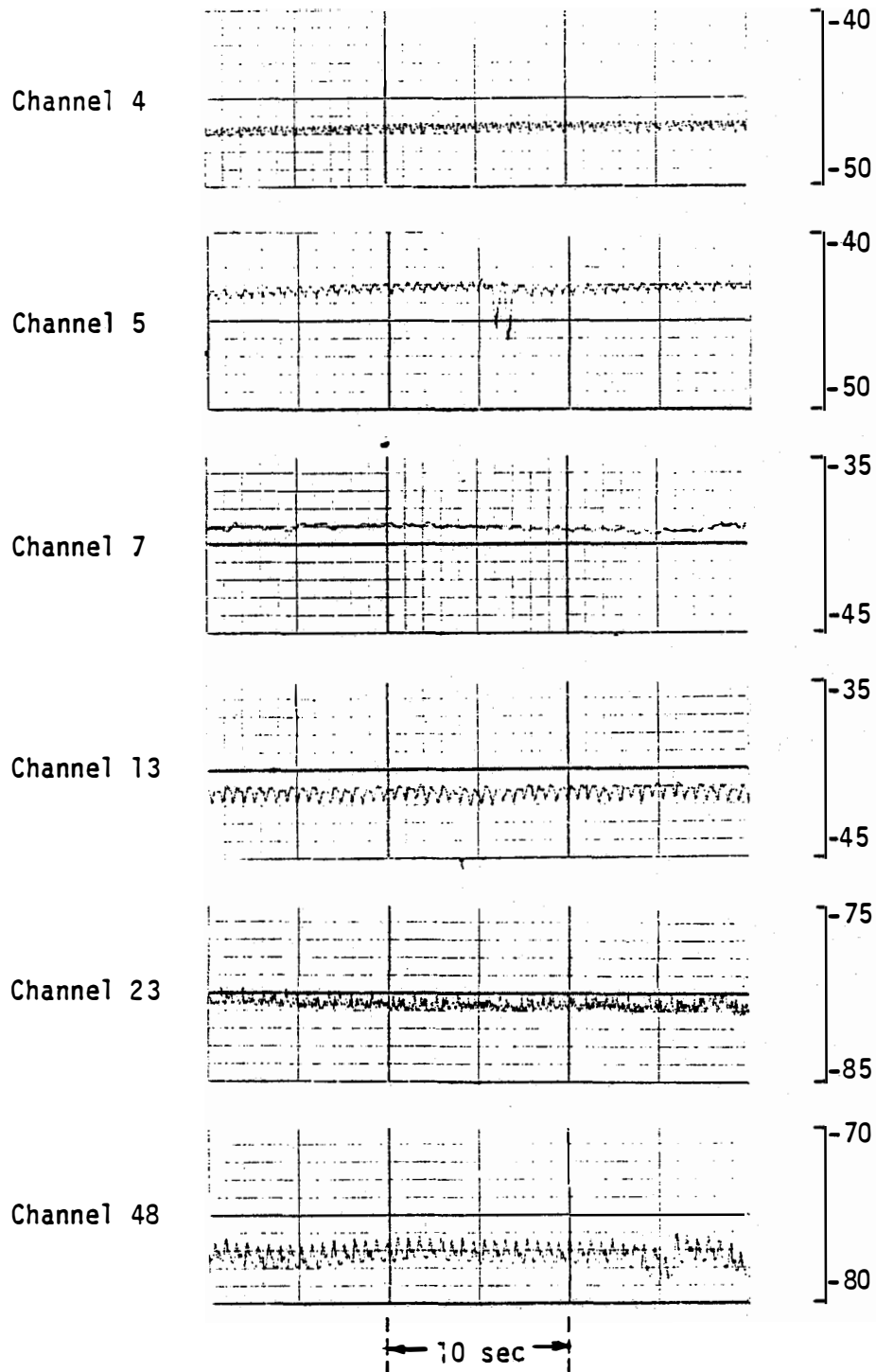


Fig. 36: P_a (in dBm) versus time at site 2.

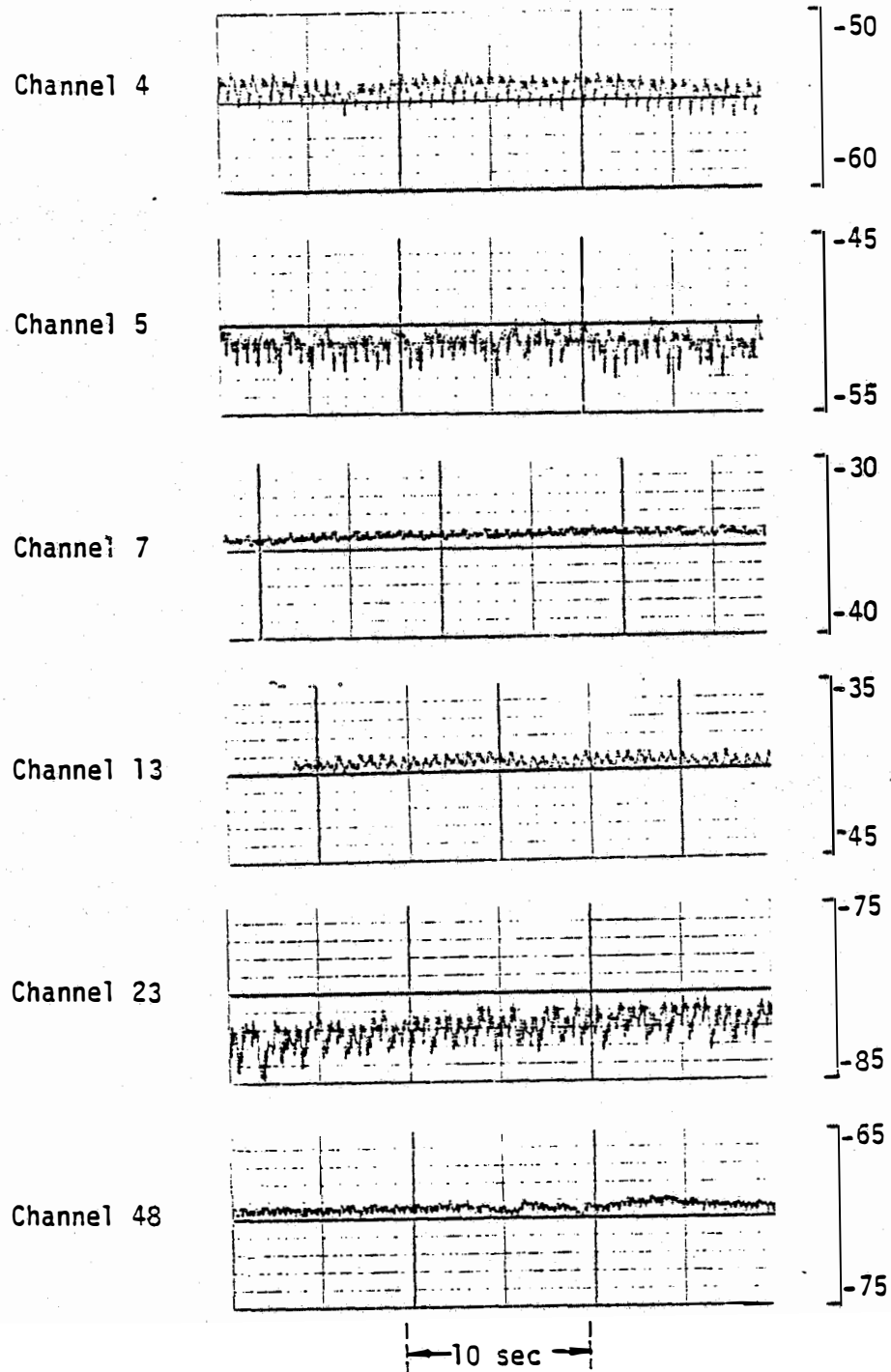


Fig. 37: P_a (in dBm) versus time at site 6.

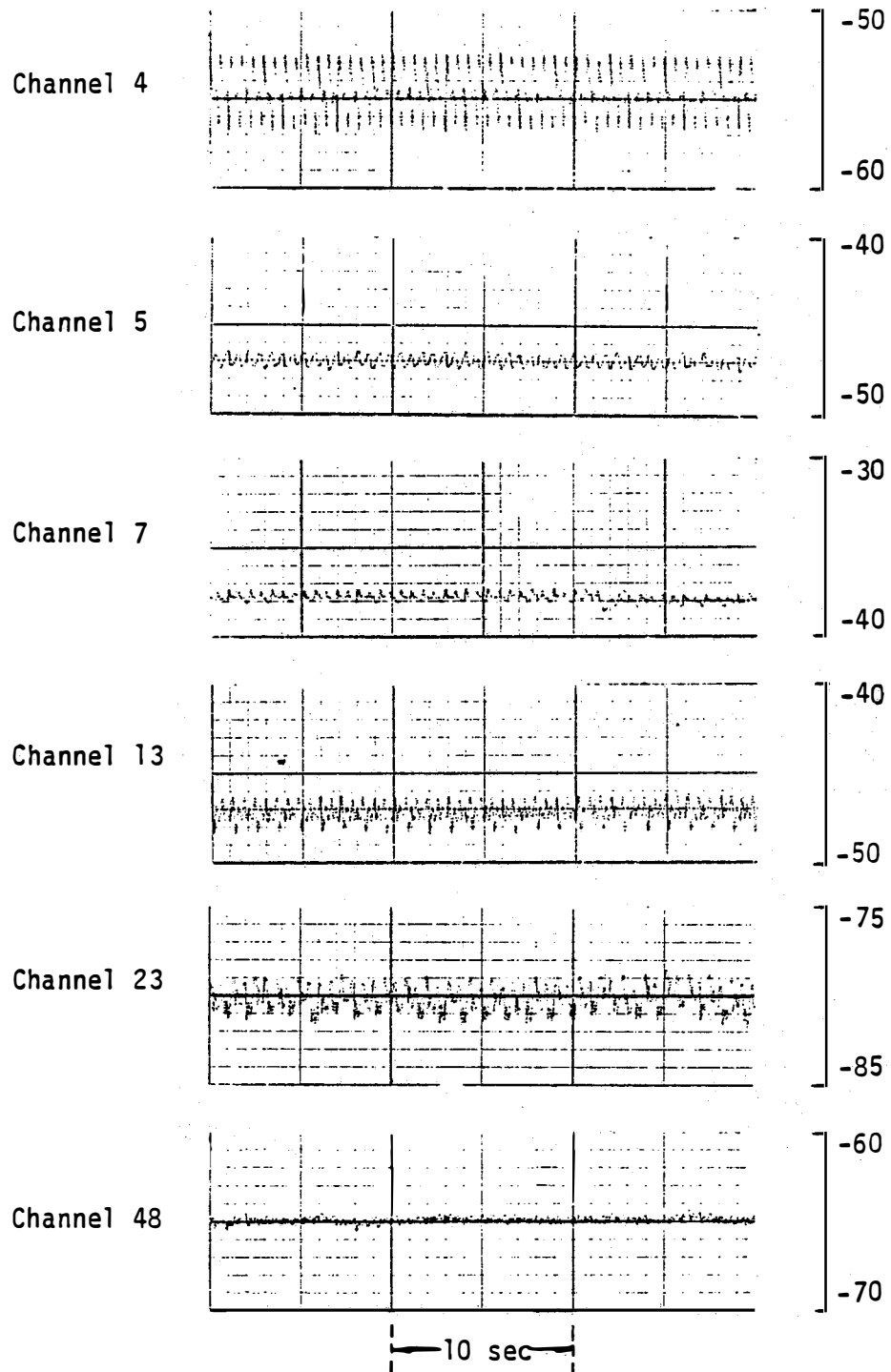


Fig. 38: P_a (in dBm) versus time at site 4.

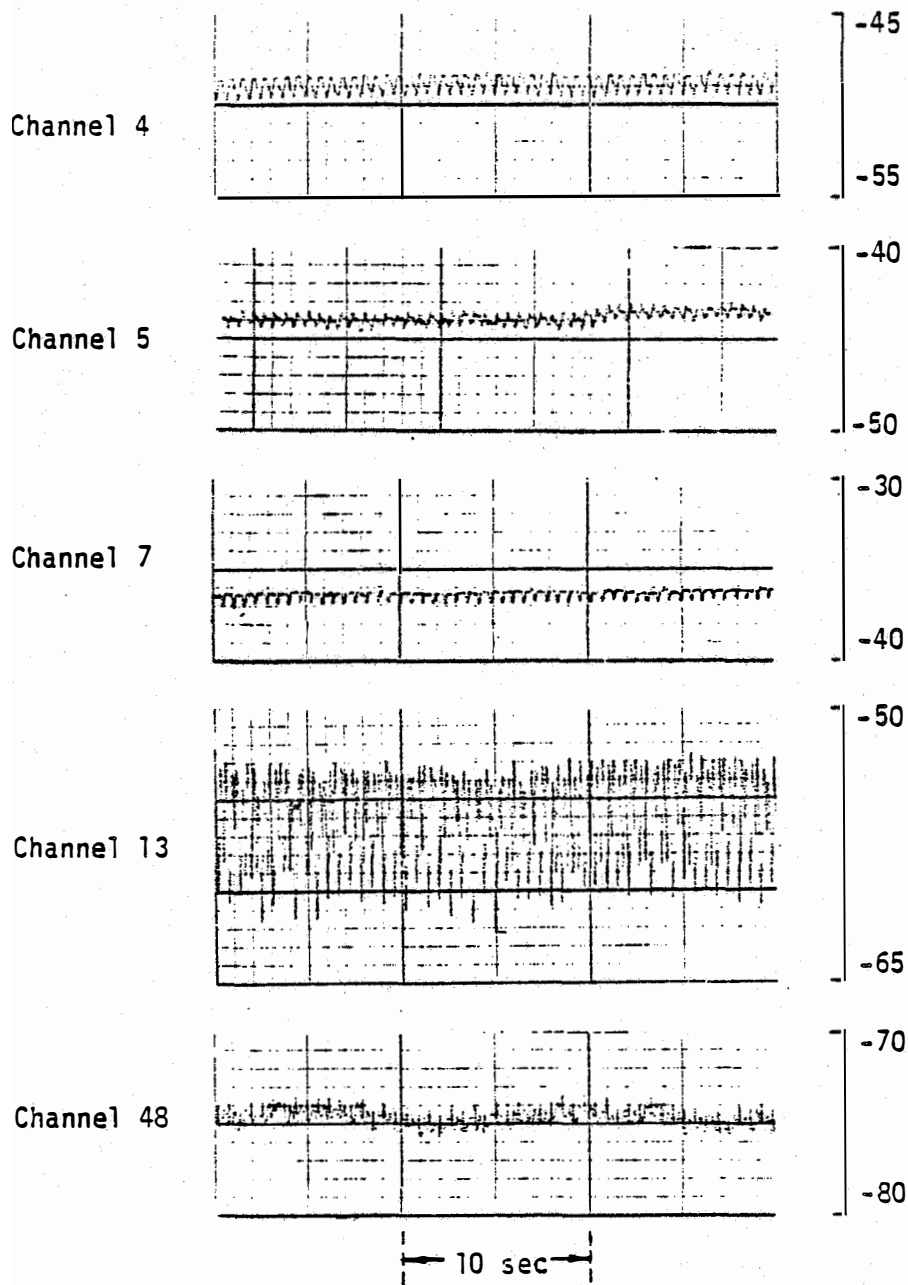


Fig. 39: P_a (in dBm) versus time at site 7.

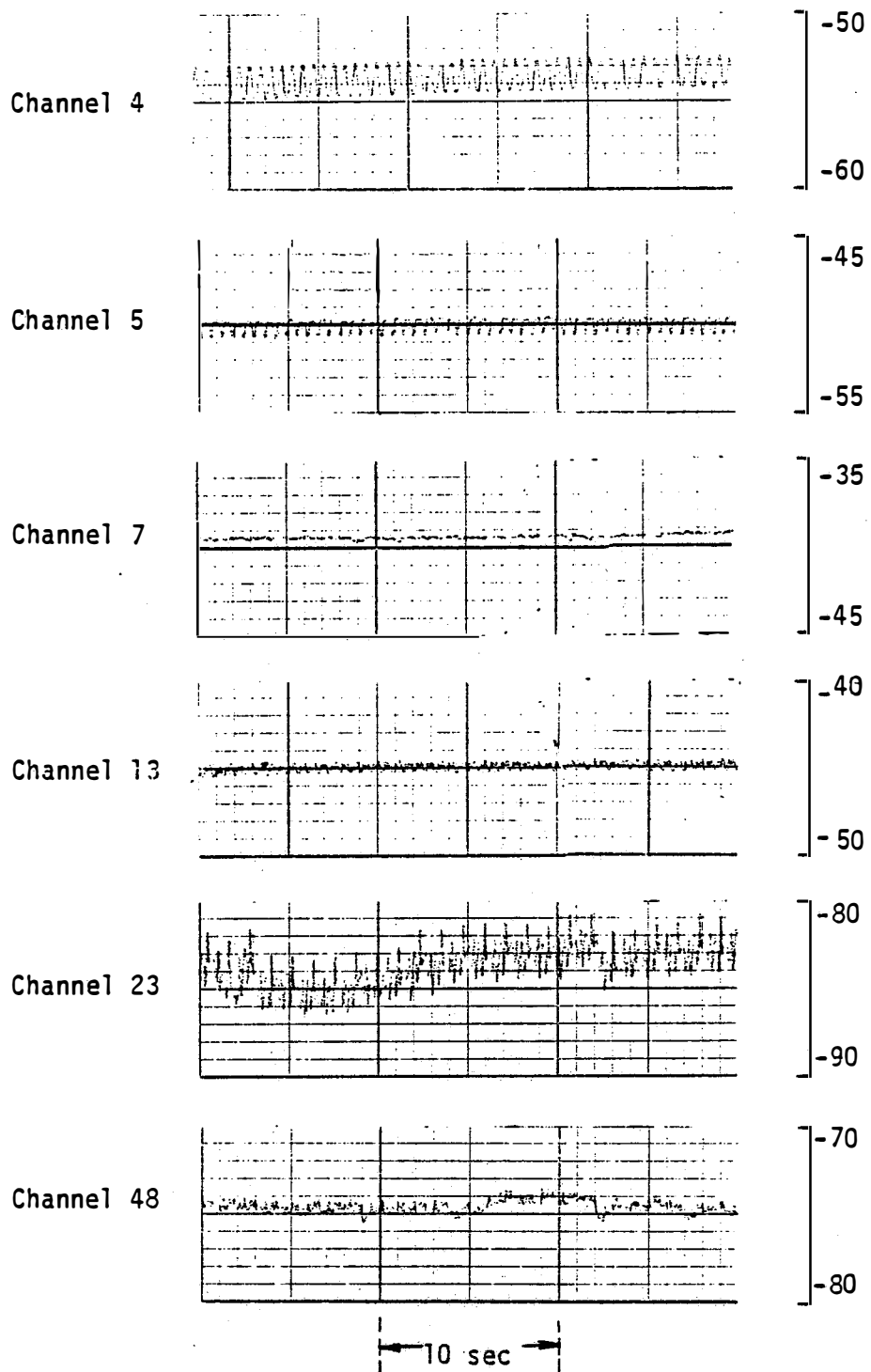
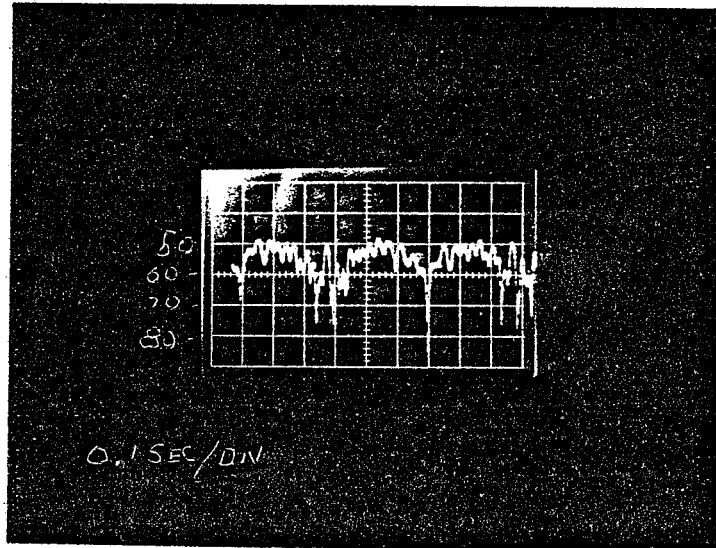


Fig. 40: P_a (in dBm) versus time at site 8.

Channel 23 made it impossible to obtain a valid recording of P_a versus time, and the largest signal variations found were on Channel 13 where the video distortion was strong and unacceptable.

The modulation waveforms in Figs. 36 through 40 appear site and frequency (or Channel number) dependent, and are more complicated than those produced by a horizontal axis WT [1,2]. They vary from almost sinusoidal to pulsed in nature, with a dominant component repeating at twice the rotation frequency of the blade. To illustrate the detailed structure, Fig. 41 is a photograph of the modulation waveform received on Channel 13 at site 7 obtained using the oscilloscope-camera combination (see Fig. 5) whose response is faster than the strip chart recorder, c.f., Fig. 39. The following features can be identified: an almost sinusoidal variation of period $0.3 \text{ sec} = T/4$ where T is the period of the blade's rotation (1.2 sec at 50.6 rpm), on top of which ride (i) small amplitude and rapidly varying noise-like sinusoids; (ii) a broad pulse 50 to 75 μs wide repeating at intervals of $T/2$; (iii) a strong narrow spike separated from this pulse by $T/4$ and repeating at $T/2$; and (iv) a pair of strong narrow spikes at the base of the pulse in (ii) and repeating at $T/2$.

From the correlation and synchronism of the signal variations Δ in Figs. 36 through 40 with the video distortion, it would appear that the distortion is produced by the broad pulses (ii) in the waveform; however, this is by no means certain. The origins of the various components in the modulation waveform are not presently understood, and until they are, it will be impossible to specify those features of a VAWT which are most responsible for TVI.



0.1 sec per horizontal division
-10 dBm per vertical division

Fig. 41: Photograph showing the modulation waveform received on Channel 13 at site 7.

6.3 Theoretical Considerations

The scattering from the rotating blades of the Darrieus modulates the total received signal, and the observed modulation waveforms are quite complicated. In addition to the periodic features whose frequencies are 2Ω and its harmonics where Ω is the radian frequency of blade rotation, there are variations from site to site and Channel to Channel, with the waveform itself varying from almost sinusoidal to pulsed in nature. The modulation is the source of the TV interference and is intimately related to the scattering produced by the Darrieus blades. In order to predict the interference and, in particular, to compare it with that of a HAWT, it is therefore necessary to develop a theory for the scattering from the blades. This has not yet been done, but some preliminary results have been obtained based on a simplified model of the scattering, and these will now be presented.

The theory assumes that in directions other than forward, the scattering is produced by two diametrically opposed portions of the blade surface a distance $2a$ apart, and the model consists of two point scatterers each having an equivalent scattering area $A/2$ separated by a distance $2a$ in a horizontal plane. The pair rotate in a horizontal plane at an angular frequency Ω about a fixed point B (see Fig. 42) which will later be identified with the phase center of the Darrieus, and are illuminated by an incident plane wave. The scattered field at the point R distance r from B is then

$$E^S(R) = \frac{AE^B}{2\lambda} \left\{ e^{ika \cos \Omega t} \frac{e^{-ikr_1}}{r_1} + e^{-ika \cos \Omega t} \frac{e^{-ikr_2}}{r_2} \right\} \quad (1)$$

where E^B is the amplitude of the incident field at B, $k = 2\pi/\lambda$ is the free space propagation factor, a time factor $e^{i\omega t}$ has been assumed and omitted, and

$$r_{1,2} = \left\{ r^2 + a^2 \mp 2ar \cos(\phi - \Omega t) \right\}^{1/2} .$$

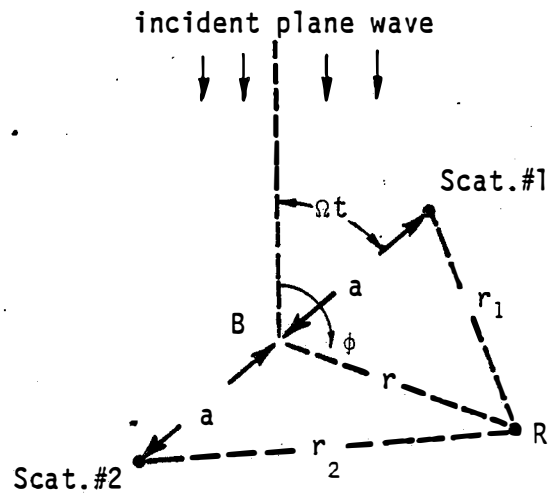


Fig. 42: Geometry for the simplified scattering model.

In the Fresnel region of a scatterer of overall dimension $2a$, $r_{1,2}$ can be approximated as

$$r_{1,2} = r \mp a \cos(\phi - \Omega t) + \frac{a^2}{2r} \sin^2(\phi - \Omega t)$$

and by following the usual procedure of neglecting the quadratic term in the amplitude factors, the expression for the scattered field becomes

$$E^S(R) = \frac{A}{\lambda r} E^B e^{-ikr} e^{i\delta(t)} f_m(\phi, \Omega t) \quad (2)$$

with

$$\tan \left\{ \delta(t) + \frac{ka^2}{2r} \sin^2(\phi - \Omega t) \right\} = \frac{a}{r} \cos(\phi - \Omega t) \tan \left\{ \rho \cos \left(\frac{\phi}{2} - \Omega t \right) \right\}$$

$$f_m(\phi, \Omega t) = \left\{ 1 - \frac{a^2}{r^2} \cos^2(\phi - \Omega t) \right\}^{-1} \left[\cos^2 \left\{ \rho \cos \left(\frac{\phi}{2} - \Omega t \right) \right\} + \frac{a^2}{r^2} \cos^2(\phi - \Omega t) \sin^2 \left\{ \rho \cos \left(\frac{\phi}{2} - \Omega t \right) \right\} \right]^{1/2}$$

and

$$\rho = 2ka \cos \frac{\phi}{2} .$$

Most of the sites were in the Fresnel (near field) region of the Darrieus, and (2) shows that the rotation produces amplitude and phase modulation with modulation functions $f_m(\phi, \Omega t)$ and $\delta(t)$ respectively. Both functions have components whose frequencies are 2Ω and its harmonics, and in the particular case of forward scattering, $\phi = \pi$, most (but not all) of the phase modulation disappears. The expression (2) simplified considerably in the far field where $r \gg a$ and $ka^2/2r \ll 1$, and we then have

$$E^S(R) = \frac{A}{\lambda r} E^B e^{-ikr} \cos \left\{ \rho \cos \left(\frac{\phi}{2} - \Omega t \right) \right\} \quad (3)$$

In the particular case of forward scattering ($\phi = \pi$), $\rho = 0$ and the blade rotation produces no modulation at all. This is unrealistic and

would not occur with a more refined model of the scattering in which, for example, the scatterers were treated as non-isotropic.

To determine the effect of the scattered field (3) on the reception of the TV signal at R, it is necessary to compute the amplitude envelope of the total (direct plus scattered) field at R and then study the influence of the various frequency components after first detection of the combined signal by the TV receiver. This has not yet been done, but as a first step it would seem reasonable to assume that the interference is primarily determined by the amplitude of the scattered field relative to the direct field at R. It was observed that the maximum interference occurred when $\phi \approx 2\Omega t$, and the resulting modulation index is

$$m = \frac{|E^S(R)|}{E^R} = \frac{A}{\lambda r} \frac{E^B}{E^R} |\cos(2ka \cos \frac{\phi}{2})| \quad (4)$$

where E^R is the amplitude of the direct field at R.

The last step is to take into account the presence of the earth and the use of a directional receiving antenna. For a plane perfectly conducting ground the extension is relatively straightforward, and if h_s and h_r are the heights above ground of the scatterers and the receiving antenna respectively, we have (see [2])

$$m = \frac{A}{\lambda r} \frac{E^B}{E^R} |\cos(2ka \cos \frac{\phi}{2})| \left| 2 \sin \left(\frac{2\pi h_s h_r}{\lambda r} \right) \right| F(B,T) \quad (5)$$

where $F(B,T)$ is the voltage response of the antenna in the direction of the WT relative to that in the direction of the transmitter. The

expression for the modulation index is similar to that obtained for a HAWT. In (5), A represents the equivalent scattering area for a Darrieus machine, and is clearly the key parameter in specifying the interference. We shall now use (5) to deduce this parameter from the measured values of the modulation index at one of the sites.

6.4 Data Analysis

Equation (5) was derived under the assumption of a receiving antenna in the far field of a scatterer of diameter $2a$. Since $a = 8.5$ m for the Darrieus, the only site which fulfills this condition is site 1 for the two lower VHF Channel frequencies. At this site $r = 132$ m, $\phi = 90^\circ$ and $h_r = 7.6$ m with $h_s = a + 4.3 = 12.8$ m. For the various Channels the antenna response functions $F(B,t)$ can be obtained from Figs. 14 through 19. With the antenna beam pointed at the WT, the signal variations Δ can be found from the P_a vs time recordings (they can also be read from Figs. 14 through 19), and the corresponding values of the modulation index derived using Fig. 20. The results are presented in Table 10, along with the values of the equivalent scattering area A computed from (5) under the assumption $E^B = E^R$, i.e., the ambient field strengths are the same at the WT and the site. The Channels for which no data are given in Table 10 are those for which there was no observable signal variation.

The ambient field strengths were not measured at the WT itself but they were measured at the eight sites, and showed considerable variation (see Table 6). It is therefore probable that $E^B \neq E^R$ at site 1, and to obtain a better estimate of E^B we have

Table 10

Equivalent area of the Darrieus obtained from the measurements
at site 1 with $E^B = E^R$, $r = 132$ m

TV Channel	λ (m)	Δ (dB)	m	F(BT)	A (m ²)
4	4.18	1.0	0.057	5.01	4.95
5	3.67	0.3	0.017	7.08	3.86
7	1.67	--	--	--	--
13	1.39	0.9	0.050	7.08	5.89
23	0.57	--	--	--	--
48	0.44	1.5	0.085	3.98	1.72

Table 11

Equivalent area of the Darrieus obtained
from measurements at site 1

TV Channel	E^B (av) (-dBm)	E^R (-dBm)	E^R/E^B	A (m ²)	$w\sqrt{2a\lambda}$ (m ²)
4	36.30	36	1.04	5.00	5.14
5	35.00	34	1.12	4.34	4.82
13	32.25	36	0.65	3.82	2.96
48	55.25	59	0.65	1.12	1.66

averaged the values measured at the four closest-in sites 5,6,7 and 8. The results of the revised calculations are shown in Table 11 where we also list the physical optics estimate $w\sqrt{2a\lambda}$ for the scattering area of a strip of width $w = 0.6\text{m}$ (= 24 inches) bent into an arc of radius a . In spite of the fact that the procedure by which the equivalent scattering area A was deduced cannot be fully justified at the two higher frequencies (site 1 was not then in the far zone of the scatterer), the agreement with the theoretical formula is amazingly good. In particular, the formula explains why A decreases with increasing Channel number, in contrast to the case of a HAWT whose scattering area is independent of frequency.

All of the other sites were in the near field of the WT on all of the TV Channels, and the simple expression (3) for the scattered field is no longer applicable. Instead of having a $1/r$ dependence, the amplitude of the scattered field now varies sinusoidally with distance as a result of the changing phase relation between the contributions from the two point scatterers, and it is not surprising that the measured signal variations differ from those predicted using (5). To illustrate this fact, the values of m deduced from the measured signal variations Δ at sites 5 and 2 (see Figs. 35 and 36) are listed in Tables 12 and 13 respectively, along with the values computed from (5) using the equivalent scattering areas from Table 11. In most instances the measured values are lower than the computed ones by a factor of 2 or more.

Table 12

Calculated and measured values of m at site 5

(r = 27 m)

TV Channel	F(BT)	m x 100 Calculated	m x 100 Measured
4	1.0	6.6	3.4
5	1.0	6.3	4.6
13	1.0	13.1	5.7
48	1.0	19.0	8.6

Table 13

Calculated and measured values of m at site 2

(r = 37 m)

TV Channel	F(BT)	m x 100 Calculated	m x 100 Measured
4	3.2	13.0	5.4
5	2.8	11.0	6.0
13	3.2	4.2	7.0
48	8.9	47.0	14.0

6.5 Comparison with a HAWT

The above analysis suggests that in directions other than $\phi = 0$ and π the field scattered by a Darrieus machine can be attributed to two specularly reflected contributions from diametrically opposite portions of the loop blade, and at the lower VHF frequencies at least, an adequate approximation to the equivalent scattering area A is provided by the physical optics estimate

$$A = w\sqrt{D\lambda} \quad (6)$$

where w and D are the blade width and blade (loop) diameter respectively. In the back and forward directions it is expected that the entire blade will contribute. We note that A decreases with increasing Channel number (or frequency) and that for the 50 kW machine at the Sandia Laboratories

$$A = 2.5\sqrt{\lambda} \text{ m}^2 \quad (7)$$

where the wavelength λ is in meters.

It is of interest to compare the TV interference produced by comparable-sized horizontal and vertical axis wind turbines, but it should be emphasized that the conclusions are only tentative. Although the present study has provided valuable information about the interference caused by a Darrieus machine, our understanding of the modulation waveforms and their effect on the video reception is less complete than for a HAWT (see [7]). The modulation waveforms caused by the rotating blades of the Darrieus are much more complicated

than those of a HAWT, but there are also similarities, e.g., significant components repeating at twice the rotation frequency of the blades.

The video distortion observed was also similar and occurred in synchronism with the repetitive pulses, and it also appears that the threshold modulation index is comparable for the two types of machine. On the assumption that the threshold is actually the same, a preliminary comparison is possible.

The rated powers of the MOD-OA and MOD-1 horizontal axis machines are 200 kW and 2 MW respectively, and since their equivalent scattering areas are [7] 12 and 40 m², it is reasonable to assume that for a 50 kW HAWT, A = 6 m². To conform with the 17 m Darrieus, the height of its rotor axis above the ground is taken to be 12.8 m. Since, to a first approximation, the interference distance is proportional to the scattering area, the distances r_V and r_H for vertical and horizontal axis machines respectively are related by

$$\frac{r_V}{r_H} = \frac{1}{w\sqrt{D\lambda A}} \quad , \quad (8)$$

and for the 50 kW machines

$$\frac{r_V}{r_H} = 0.42 \sqrt{\lambda} \quad (9)$$

The interference is therefore identical (r_V = r_H) when λ = 5.8 m, i.e., on Channel 2, but as the frequency (or Channel number) increases, the Darrieus produces progressively less interference than the HAWT, e.g., by a factor of 2 on Channel 13, and by a factor of 4 on Channel 74.

CHAPTER 7. CONCLUDING REMARKS

The interference to TV reception caused by the operating 17 m Darrieus at Albuquerque has been studied using measurements carried out at eight test sites in the vicinity of the WT. The RF sources were the commercial TV Channels 4,5,7,13,23 and 48 available locally.

The signal strengths on Channels 4,5,7,13 and 48 were quite strong and, with the WT stationary, the quality of reception was good at all sites. The Channel 23 signal was much weaker and its reception was found to be poor at all of the sites. On some of the Channels the ambient signal strengths varied considerably from site to site.

With the antenna beam directed at the transmitter to receive the maximum (primary) signal, the significant findings from the dynamic measurements with the WT rotating were:

(i) In the forward direction ($\phi = 180^\circ$), acceptable video distortion was observed on Channels 23 and 48 at a distance of 33 m from the WT.

(ii) In the backward direction ($\phi = 0$) there was no video distortion on any Channel at a distance of 37 m.

(iii) At two sites on the 90° radial 21 and 33 m from the WT, strong (unacceptable) video distortion occurred on Channel 23.

(iv) At two sites 23 m from the WT on the 45° and 135° radials, there was interference above acceptable levels on Channels 13 and 23 respectively.

When the antenna beam was directed at the WT, interference ranging from slight to violent was observed on some or all Channels at all eight test sites. The modulation waveforms produced by the rotating

Darrieus are more complicated than for a horizontal axis machine and are not yet fully understood. The waveforms varied from sinusoidal to pulsed, with significant components repeating at twice the rotation frequency of the WT. The video distortion occurred in synchronism with these components.

As with all WTs, a key factor that affects the interference is the equivalent scattering area of the machine. A simple theoretical model has been developed for analyzing the TVI produced by a VAWT like the Darrieus. Using the model and the measured data, an approximate expression for the equivalent scattering area A of the 17 m Darrieus has been derived. It is found that A is wavelength (λ) dependent and varies as $\lambda^{1/2}$. When compared with a HAWT having a similar power rating, it now appears that the Darrieus produces the same amount of interference on the lowest VHF Channel, but less on all other Channels, e.g., by a factor of 2 on Channel 13.

Overall the test program was successful. In addition to providing specific data for the Darrieus machine, it has also produced a better understanding of how the interference is produced, and yielded valuable information about the equivalent scattering area. Nevertheless, further work is required in order to predict the interference caused by a Darrieus or other VAWT with the same degree of confidence that is now possible for a HAWT. In particular,

(i) the bistatic scattering properties of Darrieus-like blades should be investigated to determine the dependence on the physical dimensions, aspect and wavelength;

(ii) the various modulation waveforms produced by the rotating blades should be studied to better understand their key features and, hopefully, to enable them to be predicted; and

(iii) those features of the modulation waveform which affect the signal after first detection by a TV receiver should be determined. The resulting theoretical model of the interference process should then be verified using on-site measurements with an appropriate VAWT.

REFERENCES

- [1] D. L. Sengupta, T.B.A. Senior and J. E. Ferris, "Television Interference Tests on Block Island, RI," University of Michigan Radiation Laboratory Report No. 014438-3-T, January 1980.
- [2] D. L. Sengupta, T.B.A. Senior and J. E. Ferris, "Measurements of Interference to Television Reception Caused by the MOD-1 WT at Boone, NC," University of Michigan Radiation Laboratory Report 018291-1-T, January 1981.
- [3] D. L. Sengupta and T.B.A. Senior, "Wind Turbine Generator Interference to Electromagnetic Systems," University of Michigan Radiation Laboratory Report No. 014438-3-F, August 1979.
- [4] Alcoa Laboratories, "Design and Fabrication of a Low Cost Darrieus Vertical Axis Turbine Systems. Phase I," ALO-4272-T1, Contract No. EM-78-C-04-4272, Aluminum Company of America, Alcoa Center, Pennsylvania 15069, June 1979.
- [5] M. H. Worstell, "Aerodynamic Performance of the 17-Meter-Diameter Darrieus Wind Turbine," SAND78-1737, UC-60, Sandia Laboratories, Albuquerque, NM 87185, January 1978.
- [6] D. L. Sengupta and T.B.A. Senior, "Electromagnetic Interference to Television Reception Caused by Horizontal Axis Windmills," Proc. IEEE, Vol. 67, No. 8, pp. 1133-1142, August 1979.
- [7] D. L. Sengupta and T.B.A. Senior, "Electromagnetic Interference by Windmills," University of Michigan Radiation Laboratory Report No. 014438-2-F, March 1978 (TID-28828).
- [8] T.B.A. Senior and D. L. Sengupta, "Wind Turbine Generator Siting and TV Reception Handbook," University of Michigan Radiation Laboratory Report No. 014438-1-T, January 1978 (C00/2846-1).
- [9] T.B.A. Senior and D. L. Sengupta, "Wind Turbine Generator Siting Handbook," University of Michigan Radiation Laboratory Report No. 014438-2-T, December 1979.